Check for updates

Plant Direct

WILEY | American Society of Plant Biologists | SEB SOCIETY FOR EXPERIMENTAL BIOLOGY

RESEARCH ARTICLE OPEN ACCESS

The Q-Warg Pipeline: A Robust and Versatile Workflow for Quantitative Analysis of Protoplast Culture Conditions

Léa Bogdziewiez[1] | Rik Froeling[2] | Patricia Schöppl[2] | Jeanne Juquel[3] | Ioanna Antoniadi[1] | Vladimìr Skalický[1] | Ambroise Mathey[1] | Jacques Fattaccioli[4,5] | Joris Sprakel[2] | Stéphane Verger[1,3]

[1]Umeå Plant Science Centre (UPSC), Department of Forest Genetics and Plant Physiology, Swedish University of Agricultural Sciences, Umeå, Sweden | [2]Laboratory of Biochemistry, Wageningen University and Research, Wageningen, the Netherlands | [3]Umeå Plant Science Centre (UPSC), Department of Plant Physiology, Umeå University, Umeå, Sweden | [4]Pasteur, Département de Chimie, Ecole Normale Supérieure, PSL Université, Sorbonne université, CNRS, Paris, France | [5]Institut Pierre-Gilles de Gennes Pour la Microfluidique, Paris, France

Correspondence: Stéphane Verger (stephane.verger@umu.se)

Received: 11 March 2025 | **Revised:** 13 June 2025 | **Accepted:** 19 June 2025

Funding: This work was supported by Vetenskapsrådet (VR) (2020-03974), Novo Nordisk Fonden (NNF) (NNF21OC0067282), Aforsk (20-502), Knut och Alice Wallenbergs Stiftelse (Knut and Alice Wallenberg Foundation) (2022.0029, 2016.0352, and 2020.0240), Vetenskapsrådet (VR) (2021-04938), TopSector TKI Horticulture and Starting Materials (TU202312), EC | European Research Council (ERC) (101000981),

Kempestiftelserna (Kempe Foundations) (SMK21-0041), VINNOVA (Swedish Governmental Agency for Innovation Systems) (2016-00504), and Bio4Energy.

Keywords: *Arabidopsis thaliana* | cell wall | fluorescence | protoplasts | quantification | recovery | regeneration | viability

ABSTRACT

Single cells offer a simplified model for investigating complex mechanisms such as cell–cell adhesion. Protoplasts, plant cells without cell walls (CWs), have been instrumental in plant research, industrial applications, and breeding. However, because of the absence of a CW, protoplasts are not considered "true" plant cells, making them less relevant for biophysical studies. Current protocols for CW recovery in protoplasts vary widely among laboratories and starting materials, requiring lab-specific optimizations that often depend on expert knowledge and qualitative assessments. To address this, we have developed a user-friendly streamlined workflow, the Q-Warg pipeline, which enables quantitative comparison of various conditions for CW recovery post-protoplasting. This pipeline employs fluorescence imaging and tailored processing to measure parameters such as morphometry, cell viability, and CW staining intensity. Using this approach, we optimized culture conditions to obtain single plant cells (SPCs) with recovered CWs. Additionally, we demonstrated the robustness and versatility of the workflow by quantifying different fluorescent signals in protoplast suspensions. Overall, the Q-Warg pipeline provides a widely accessible and user-friendly solution for robust and unbiased characterization of protoplasts culture. The quantitative data generated by the pipeline will be useful in the future to decipher the mechanisms regulating protoplast viability and regeneration.

1 | Introduction

Multicellular organisms are made of millions or trillions of cells coming together in complex tissues with heterogeneities at several scales. While these heterogeneities characterize the form and functions of those tissues, they often complicate our understanding of biological mechanisms occurring within them. For instance, studying the phenomenon of cell–cell adhesion in the tissue context is complex because tissue topology, cell geometry, and cell–cell interface heterogeneities can have major confounding effects on the apparent strength of cell adhesion (Bidhendi and Geitmann 2016). On the contrary, working with single cells provides a strongly simplified framework to study cell–cell interaction (Atakhani et al. 2022). Beyond

This is an open access article under the terms of the Creative Commons Attribution-NonCommercial License, which permits use, distribution and reproduction in any medium, provided the original work is properly cited and is not used for commercial purposes.

© 2025 The Author(s). *Plant Direct* published by American Society of Plant Biologists and the Society for Experimental Biology and John Wiley & Sons Ltd.

the example of adhesion, such consideration applies to a large spectrum of biological questions, which explains why cell cultures are such a widely used model system in animal sciences (Verma et al. 2020). However, when it comes to studying plants, "single plant cell cultures" do not really exist. It is possible to cultivate cells in vitro under the form of microcalli, which are small clusters of cells arising from division events and thus not real single cells (Pesquet, Wagner, et al. 2019; Krasteva et al. 2021). It is also possible to isolate and study protoplasts (see further details below; Mukundan et al. 2025), which are effectively single cells but lack the cell wall, a crucial component of plant cells that controls their shape, mechanics, adhesion, and growth and plays major roles in signaling, defense, and cell-to-cell communication (Yokoyama, Shinohara et al. 2014; Anderson and Kieber 2020; Cosgrove 2024; Anderson and Pelloux 2025). It would thus be particularly useful for the plant science community to establish an approach to generate single plant cell (SPC) populations to use them as a new model system. One possibility is to start by extracting protoplasts and letting them recover their cell wall. The challenge lies in identifying culture conditions that promote strong and homogeneous cell wall recovery while ensuring minimal cell division and high cell survival rate over several days.

A protoplast is a plant cell without its cell wall (CW, term introduced by Hanstein in 1880). In 1892, the first isolation of protoplasts was successfully conducted by Klercker (Eine Methode zur Isolierung lebender Protoplasten/von John Af Klercker 1892). In 1970, Nagata and Takebe regenerated a full plant from tobacco leaves protoplasts (Nagata and Takebe 1970). Protoplasts have proven their usefulness not only in plant research to study various cellular processes such as cell division, cell wall synthesis, or cell differentiation (Jiang et al. 2013; Yokoyama, Kuki, et al. 2016; Pasternak, Lystvan, et al. 2020; Gilliard et al. 2021) but also in industry for metabolites production (Xu et al. 2022). They are also employed as a breeding technology because a whole plant can be regenerated from genetically transformed protoplasts (Reed and Bargmann 2021; Reyna-Llorens et al. 2023; Mukundan et al. 2025). Furthermore, recent development of non-transgenic genome editing with CRISPR/Cas9 and ribonucleoproteins (Yue et al. 2021; Laforest and Nadakuduti 2022) has renewed the interest in protoplasts.

Despite more than a century of research, it is still challenging to work with protoplasts as exemplified by the large number of protocols for protoplast extraction and tissue/plant regeneration that exist (Table S2). The first step of extracting the protoplasts from a plant tissue is relatively straightforward and has been done from various plant species (Kumari 2019). Most protocols use enzymatic digestion of the CW to release protoplasts. As the CW composition can vary from one tissue to another, enzymes must be carefully selected (Mukundan et al. 2025). Once the protoplasts are isolated, the first challenge is to find the right conditions to keep them alive. Without their CW, protoplasts are fragile and cannot withstand physical/mechanical stress. They require high osmolarity and low to no agitation to avoid bursting before the cell wall is recovered. However, the subsequent steps leading to CW recovery and cell division, toward tissue regeneration, appear to be the most challenging to establish and optimize (Xu et al. 2022; He et al. 2025).

Plant cells are normally surrounded by their CW, which is mainly composed of cellulose and a matrix of other polysaccharides deposited outside of the plasma membrane (Cosgrove 2024). The first challenge for the protoplasts to rebuild their CW is to retain newly synthesized CW polysaccharides at their surface. Matrix polysaccharides are secreted from the Golgi and may at first simply end up in the liquid medium (Oda et al. 2020; Hoffmann et al. 2021). Similarly, cellulose is synthesized at the surface of the plasma membrane and may primarily be extruded outward rather than sticking to the membrane (Paredez et al. 2006; Purushotham et al. 2020). Yet, those cellulose microfibrils are tethered to the membrane via the cellulose synthase complex and may act as traps for secreted polysaccharides such as xyloglucans (Park and Cosgrove 2012). It is also possible that Golgi-synthesized polysaccharides already interact with membrane-bound protein before secretion and thus remain partially attached to the surface upon secretion (McKenna et al. 2014; Fruleux et al. 2019). Furthermore, glycosylphosphatidylinositol (GPI)-anchored arabinogalactan proteins, with their extensive glycosylation and anchorage at the membrane, may be one of the players contributing to retain polysaccharides at the membrane surface (Tan et al. 2013; Leszczuk et al. 2023). Over time, the cell wall polysaccharides may begin to accumulate in patches, while the cellulose could develop into a network that will then efficiently retain additional CW deposits on the cell surface (Tagawa et al. 2019). Ultimately, a rather uniform CW may be recovered around the protoplast (Tagawa et al. 2019). However, this scenario remains very speculative, as the mechanisms of CW recovery are still largely unknown.

Although it seems that CW recovery would be almost inevitable over time, in reality, depending on the growth conditions, many protoplasts are unable to recover their CWs and instead remain as seemingly wall-less protoplasts (Xu et al. 2022). Some protocols aiming to regenerate whole plants from protoplasts take the approach of embedding the protoplasts into a gel (alginate) to help the CW recovery and callus formation (Damm and Willmitzer 1988; Masson and Paszkowski 1992; Jeong et al. 2021; Sakamoto et al. 2022). This embedding likely allows the full retention of secreted polysaccharides at the protoplast surface and thus an efficient recovery of the CW, paving the way for the first cell division, microcalli formation, and later on tissue regeneration. While CW recovery is a crucial step, for applications aiming toward tissue regeneration, it is generally enough that small proportions of the protoplasts recover their CW (Jeong et al. 2021). These cells can then divide, proliferate, and ultimately constitute the majority of the cell culture over the protoplasts that did not recover their CW. It is likely for those reasons, along with protoplast embedding methods, that optimizing protoplast CW generation has not been a major research focus in the past. Yet, with the renewed interest in biomechanical studies in plants, our intention is to obtain large, homogeneous populations of SPCs with "native" CWs (e.g., to test their adhesion properties) that can be manipulated as individual cells. Hence, we aim for the majority of the protoplasts to recover their CWs. Embedding is not an

24754455, 2025, 7, Downloaded from https://onlinelibrary.wiley.com/doi/10.1002/pld3.70090 by Umea University, Wiley Online Library on [21/07/2025]. See the Terms and Conditions (https://onlinelibrary.wiley.com/terms-and-conditions) on Wiley Online Library for rules of use; OA articles are governed by the applicable Creative Commons License

option as it either traps the cells, preventing manipulation, or may "contaminate" the CW surface with polymers from the gelling agent.

Several methods and protocols have been developed and claimed to yield high CW recovery (Table S2). Preliminary results in our hand did not yield CW recovery at levels comparable to the literature values. Indeed, the existence of protocols with substantial variations in medium composition and growth conditions suggests that CW recovery efficiency may be highly lab dependent. A protocol that works optimally in a given lab and its local conditions may not work efficiently in another lab. Parameters like temperature, local water parameters, air moisture level, local provider of chemicals, and medium components could have direct or indirect effects on the medium and growth environment of the cells and may be challenging to track down. Instead, ideal medium and growth conditions may need to be tested and optimized in each lab. Furthermore, medium optimization is generally required when it comes to different species, varieties, or even different tissues within the same species (Reed and Bargmann 2021). Surprisingly, from a non-expert point of view, the approaches to optimize in vitro culture conditions almost appear as an art, often based on qualitative observations and relying on the skills and expertise of exceptional researchers and research groups with decades of experience. Most studies that document their optimization procedure report qualitative observations or largely manual measurements because of the lack of widely available quantitative and high-throughput methods. From the literature gathered in Table S1, in most cases, optimization is based on microscopy observations without quantification or with manual scoring of the protoplast viability (e.g., Schirawski et al. 2000; Pasternak, Paponov, et al. 2021). This implies that the experimenter must already have a good experience of what a "good culture" looks like as stated in the largely cited protocol of Yoo et al. (2007). In theory, fluorescence-activated cell sorting (FACS) offers a high-throughput, quantitative, and unbiased approach to objectively characterize cells after protoplasting (Antoniadi et al. 2022), but it unfortunately remains rarely accessible in many research labs and usually also requires advanced skills and expertise.

Here, we present an accessible workflow, developed to quantify cell viability and CW recovery after protoplasting. Using widely available fluorescence imaging and a custom image processing workflow, the quantitative cell wall regeneration (Q-Warg) pipeline reports several parameters of a cell or protoplast suspension, such as morphometry (size, circularity, etc.), viability, and CW staining intensities (see additional files or https://github.com/VergerLab/Q-Warg for user guide, protocol, and scripts). This allows quick screening of numerous parameters to optimize and compare them with quantitative data. Thanks to this pipeline, we could optimize conditions to obtain SPCs derived from protoplasts. We also further investigated approaches to select a homogeneous population of SPCs. To test the robustness of our workflow, we used it to optimize high cell viability and fast CW recovery in media designed to accelerate subsequent cell division and tissue regeneration. Finally, we demonstrate the versatility of the workflow by using it to quantify the proportion of protoplasts containing chloroplasts after protoplast extraction from seedlings. Overall, we provide a new approach and set of tools to improve efficiency, accuracy, and reproducibility when working with protoplasts, their viability, and their CW recovery and demonstrate their usefulness in different scenarios.

2 | Results and Discussion

2.1 | Q-WARG: Quantitative Cell Wall Regeneration Pipeline

The Q-Warg pipeline (Quantitative cell WAll ReGeneration) was originally designed as a quantitative screening approach to optimize in vitro culture conditions for cell viability and CW recovery after protoplasting. Note that throughout the manuscript, we use the term recovery instead of regeneration to avoid confusion with the process of protoplast regeneration that implies the growth of a whole plant from one protoplast. The screening is based on brightfield and widefield fluorescence imaging, followed by quantitative image processing and data analysis (Figure 1). Such quantitative analysis helps screen optimal culture conditions in a more objective and trackable way. Semi-automated imaging along with batch image processing and quantitative analysis makes the process high throughput compared to classical manual quantification or qualitative observation. Compared to flow sorting methods, our approach uses tools widely available in research labs or core microscopy facilities (fluorescence light microscope), which makes it accessible to most research labs without specialized equipment. In this section, we describe the main principles of this workflow, key considerations we applied during its development, as well as considerations for its usage. All the computational components of the workflow are available as Supporting Information and on a GitHub repository (for the latest updates and potential bug fixes) along with a detailed protocol, user guide, and tutorial videos (https://github.com/VergerLab/Q-Warg, additional Files 1–5).

Sample preparation (Figure 1A–D): Depending on the aim of the experiment, this step might differ. Protoplasts may be extracted from various tissues, leading to differences in the extraction method (Method S1 and Tables S1 and S2). After extraction and/or cultivation (Figure 1A–C), the protoplasts or cells viability can be assessed by fluorescein-diacetate (FDA) staining and their CW recovery by Calcofluor staining (Figure 1D). Those dyes are widely used to image cell viability and CW and have the advantage of being very quick to stain. They can also be imaged with brightfield microscopy to estimate their size and sphericity. Thus, in this workflow, we use co-staining with Calcofluor and FDA and image the cells with brightfield and widefield fluorescence microscopy to acquire three-channel images: brightfield, FDA, and Calcofluor (Figure 1G). Note that alternative staining for cell viability or CW could also be used, for example, CarboTrace or CarboTag for CW (Besten et al. 2025) or intrinsic fluorescent markers for viability (Huh et al. 2025). In particular, it is important to consider that while Calcofluor is the most commonly used dye for this application, it shows a dual affinity to both cellulose and callose (Sasamoto et al. 2003; Matsuo et al. 2014; Tagawa et al. 2019). Cellulose staining with Calcofluor is generally homogeneous but weaker than the more patchy and bright staining of callose. A double staining with aniline blue and a cellulose dye (e.g., CarboTrace rather than Calcofluor

24754455, 2025, 7, Downloaded from https://onlinelibrary.wiley.com/doi/10.1002/pld3.70090 by Umea University, Wiley Online Library on [21/07/2025]. See the Terms and Conditions (https://onlinelibrary.wiley.com/terms-and-conditions) on Wiley Online Library for rules of use; OA articles are governed by the applicable Creative Commons License

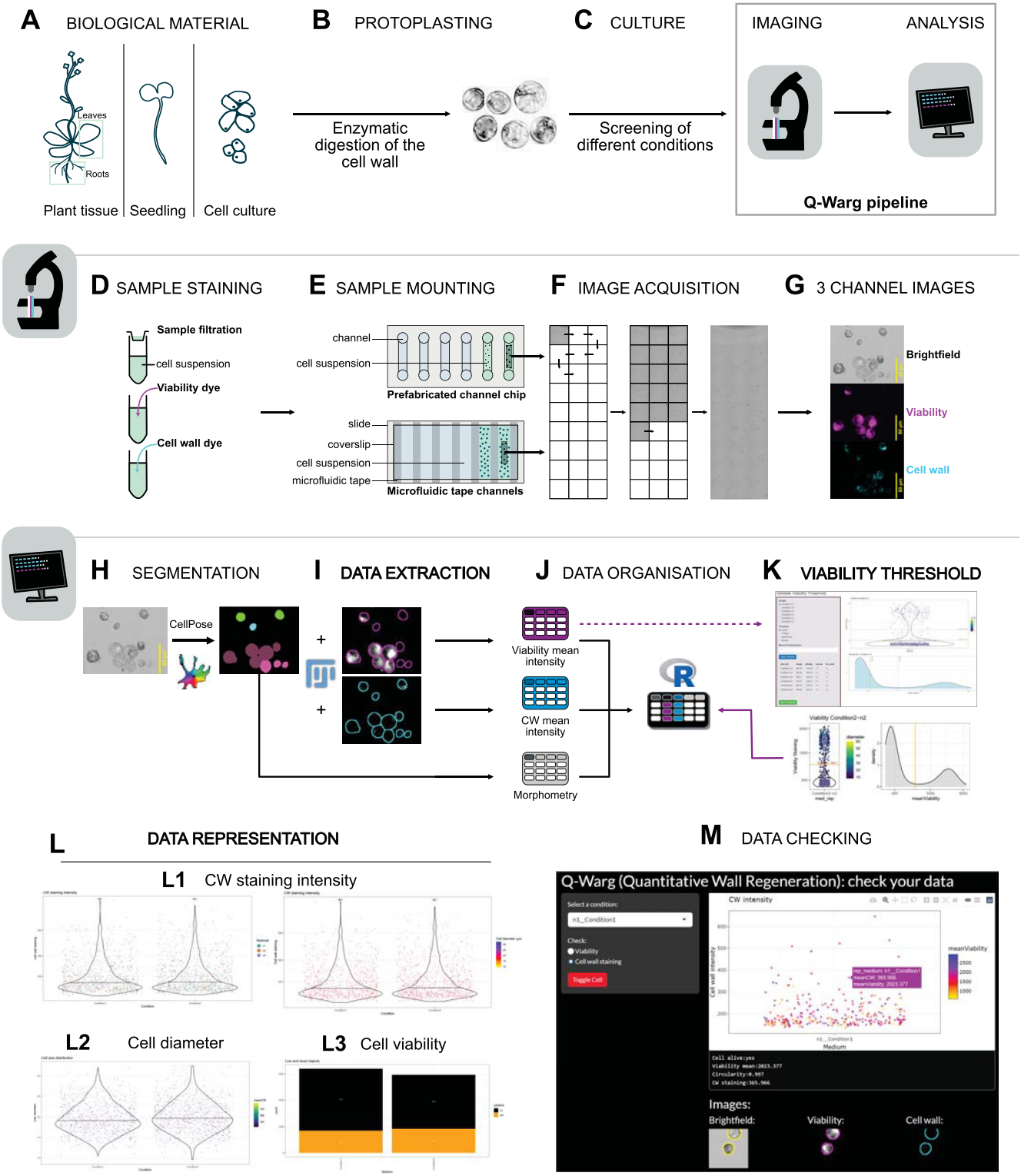

FIGURE 1 | Legend on next page.

to avoid fluorescence excitation and emission overlap) could help distinguish the callose from the cellulose (Tagawa and Kondo 2018). Depending on the aim of this study, staining might not be required (e.g., for morphometry measurements like size or circularity or intrinsic fluorescent markers).

High-throughput imaging (Figure 1E–G): For accurate quantitative analysis and high throughput of this workflow, it is useful to be able to image many cells at a time. Imaging plant cells in suspension as they are found after protoplasting and culture can be challenging for several reasons. Simply mounting the cells between slide and cover slip often leads to the cells being physically compressed and bursting. On the other hand, leaving the cells freely floating in a glass bottom dish leads to cells floating around at different focal planes, potentially overlapping and moving around during microscope

24754455, 2025, 7, Downloaded from https://onlinelibrary.wiley.com/doi/10.1002/pld3.70090 by Umea University, Wiley Online Library on [21/07/2025]. See the Terms and Conditions (https://onlinelibrary.wiley.com/terms-and-conditions) on Wiley Online Library for rules of use; OA articles are governed by the applicable Creative Commons License

FIGURE 1 | Overview of the Q-Warg screening pipeline. Q-Warg pipeline to screen and optimize protoplast culture conditions for viability and CW recovery after protoplasting. Panels describe each step from the experimental stage to the analysis. (A–C) Description of the experimental procedure in the wet lab. (A) Starting biological material can be any plant tissue. (B) Cell wall from tissue is digested by enzymes to release protoplasts. Protoplasting protocols depend on the plant tissue. (C) Protoplasts are cultivated in different conditions to be compared. Following a period of culture, the cell suspension is imaged and analyzed. (D–G) Description of the imaging process proposed in the Q-WARG workflow. (D) Sample staining for viability (in this paper, FDA was used) and cell wall staining (Calcofluor). (E) Sample is mounted in prefabricated channel chips (loaded in the entry of the channel with a micropipette) or in microfluidic tape channels: Microfluidic channels maintain a distance between the slide and the coverslip to avoid crushing the cells. Cell suspension is loaded by capillarity. (F) Image acquisition using the microscope tiling system. Large imaging by stitching multiple low-magnification images to cover a large part of the sample. (G) Three-channel images are recorded: brightfield, viability, and cell wall. (H–M) Description of the analysis process proposed in the Q-WARG workflow. (H) Segmentation based on the brightfield image using CellPose (cyto3 model). (I) ImageJ macro using MorpholibJ plugin to extract data from fluorescent images based on the label image and morphometry information. (J) Data tables are combined and organized, thanks to an Rscript to be ready for analysis. (K) Viability threshold based on the viability staining is applied on the data to analyze only the living objects in the cell suspension. (L) Data plots: (L1) cell wall staining intensity for all conditions, the color gradient shows the cell size. (L2) cell diameter for all conditions, the color gradient shows the cell wall intensity. (L3) Cell viability proportion and living cells count. Orange shows the living cells, and black shows the dead objects. (M) Data checking in Shiny app to make the link between quantitative data in the plot and images.

stage movement. All those issues would lead to complications during cell segmentation and fluorescence intensity quantification. Thus, to limit such issues, we used either prefabricated microfluidic channel chips (μ-Slide VI 0.4; Ibidi) or microfluidic tape (S5005DC, Adhesive Applications) between microscopy glass slide and cover slip to re-create microfluidic chip-like channels (Figure 1E). Loading cells in such devices is practical because cells spread out evenly and remain on a similar focal plane without being compressed, and because of the low volume of liquid, no flux is created during stage movements, so cells stay in place during imaging. Thanks to this approach, it is then possible to semi-automatically acquire large tile images with the motorized stage of the microscope (Figure 1F). Here, we used 3×9 (27) image tiles acquired with a 10× objective to keep a good balance between resolution and field of view. This generally allows the imaging of 1000–5000 cell-like objects per scan (depending on the original sample density, usually 10^5 to 10^6cells/mL), but the workflow is not limited in this respect and can process smaller or larger tile scans or single images at different resolutions and magnifications. Image tiles can also be acquired manually and stitched computationally afterwards for microscopes without motorized stages.

Quantification (Figure 1H,I): Once images are acquired, they can be used to quantify cell morphology, viability, and CW recovery. The first step of the analysis is to segment the cells from the brightfield channel image. We used CellPose (cyto3 pretrained model; Stringer and Pachitariu 2025) to obtain the label images, containing individually labeled masks for each individually segmented cell or cell-like object (Figure 1H). Note that any other segmentation method may be used at this step as long as the output is (or is made) compatible with the rest of the workflow (Method S2). We then developed a Fiji macro to extract data from the label image and the corresponding fluorescence channels (Figure 1I). In this macro, we use the plugin MorpholibJ (Legland et al. 2016) to quantify several morphometric parameters (including cell size and circularity) from the segmented labels, as well as to measure the mean signal intensity for the viability and CW fluorescence channels. The macro generates three data tables containing information about the morphometry, viability signal intensity, and CW signal intensity.

Analysis (Figure 1J,K): We conceived an R-based pipeline (R notebook) for data processing and visualization (Figure 1J–L). From the three data tables generated by the Fiji macro, we first use the R script to combine the information in a single table (Figure 1J). Because many segmented cell-like objects may not be cells or be alive, we use the FDA staining value to screen the segmented dataset and keep only what can be considered as living cells based on FDA staining intensity. Because of the quantitative nature of the analysis, the value of the signal quantified for viability and CW is not binary. There may also be heterogeneities of background signal and noise acquired from one image to the next. Thus, even dead cells may appear to have a background level of fluorescence as quantified by the workflow. Nevertheless, we generally observe a clear bi-modal distribution of fluorescence signal for FDA staining, with one low fluorescence intensity peak corresponding to dead cells and a higher intensity peak for live cells (Figure 1K). For unbiased analysis, the workflow allows the use of automated thresholding techniques to differentiate between dead and living cell populations. On our samples, Huang and Triangle methods were the most accurate, but other thresholding algorithms can also be used, such as MaxEntropy. It is noteworthy that the algorithms consistently identify a threshold, even in scenarios where the entire cell population falls into a single category (typically all dead). Consequently, there is a potential for misclassification, where a subset of cells might be wrongly categorized as viable in a predominantly nonviable population. To address this limitation, we developed an R-based Shiny application (Figure 1K) that facilitates user intervention in the thresholding process. This tool allows for the selection of the most appropriate automated method or the application of a manual threshold. However, it is crucial to emphasize that any manual threshold adjustment must be applied judiciously to maintain data integrity and avoid introducing bias into the analysis. To further avoid having false positives, like debris that are close to a living cell and are illuminated by the FDA staining of this cell, the workflow also applies a cell circularity filter. Indeed, the isolated living cells are generally very spherical (circularity close to one) as they recover their CW without environmental pressure (in suspension) while debris have various shapes. Based on preliminary observations, we chose a high circularity index (0.9) to discriminate single cells from debris and cell aggregates.

24754455, 2025, 7, Downloaded from https://onlinelibrary.wiley.com/doi/10.1002/pld3.70090 by Umea University, Wiley Online Library on [21/07/2025]. See the Terms and Conditions (https://onlinelibrary.wiley.com/terms-and-conditions) on Wiley Online Library for rules of use; OA articles are governed by the applicable Creative Commons License

Results representation (Figure 1L): The processed and filtered data are then plotted (Figure 1L). The first representation shows the CW intensity for each CW recovery condition tested, where the color gradient of the dots represents the size of the cells (Figure 1 L1). The number of living cells in each condition is noted at the top of the graph. The second plot shows the size of the cells, where the color gradient of the dots represents CW staining intensity (Figure 1 L2). Both plots are also saved with the color of the dots representing each experimental replicate. The last plot shows the proportion of living cells compared to dead cell-like objects (Figure 1 L3). While viability staining data usually show a clear bimodal distribution from which we can define a threshold for dead versus alive, CW intensity rarely shows such a clear distribution. Thus, contrary to what is usually described in publications reporting qualitative CW recovery from protoplasts, this pipeline does not output a binary yes/no answer for CW recovery. We believe that this is a more accurate output that better reflects the progressive nature of CW recovery as opposed to the more binary nature of cell viability.

Inspection (Figure 1M): Because this workflow segments and quantifies in batch thousands of cells at a time, there is always a risk of inaccurate segmentation or signal quantification leading to errors and biases in the final analysis. For instance, an incorrectly segmented cell could encompass a brightly stained CW debris, thus incorrectly assigning a high CW recovery value to that cell. With regular plots, it is nearly impossible to trace back a specific point in a plot to the corresponding cell in the raw image from which data were extracted to check the validity of the quantification. We thus aimed to develop a tool that would allow us to interactively check the dataset from the plotted data. We developed a Shiny app (R) making use of the plotly library (https://plotly.com/r/; Figure 1M) where we can choose which condition to observe and look at the cells individually by browsing through the plot. This allows us to check if the highest points are indeed real living cells or debris highly stained with Calcofluor. It is also possible to randomly check points to ensure that the value reported fits what a user can see in the microscopy image as well as if the segmentation has been done properly.

Advantages, limitations, and versatility: With the Q-Warg pipeline, many conditions to maintain a protoplast culture and recover CWs can be rapidly screened at once. It can be used after any protoplasting method and is not limited to the experimental conditions described here. Multiple parameters can be tested at once and compared quantitatively based on automatized measurements, eliminating the bias of phenotypical/qualitative observations. The workflow requires fluorescence images of the cell suspension as input. Those images can be acquired with any fluorescent microscope as long as the images can be converted to TIFF format, making this pipeline usable by most of the labs. The possible low sensitivity of widefield fluorescence microscopes can be one downfall compared to techniques that allow high detection of low signals such as FACS. Using a confocal microscope can improve the detection of such low signals but requires acquisition of Z-stacks instead of one-plane image to get signal from the entire surface of cells. Additional image processing scripts can be used to generate 2D Z-projections in batch and facilitate image formatting from the microscope format into TIFF (see https://github.com/VergerLab/Q-Warg for an example). All software (CellPose, Fiji, and RStudio) are free and do not require high computational power nor specific operating system (can be used on Windows, Linux, or MacOS). Despite our efforts to make the pipeline as user-friendly as possible, three different software packages are required to do the analysis, which can be overwhelming in the first place. Yet, once the user is familiar with the workflow, making modifications becomes straightforward, allowing for a high degree of adaptability within the pipeline. As a proof of concept, for this study, the Q-Warg pipeline was successfully used by two different teams, using different imaging systems (epifluorescence microscope Leica Dmi8 and confocal microscope Nikon ECLIPSE Ti2) and biological material (root cell culture, PSB-D, and seedlings). In this paper, special attention is paid to CW recovery after protoplasting. Viability alone is also a crucial parameter monitored after any type of protoplasting-based experiments. This can be quantified in an accurate and traceable way by our pipeline. As this pipeline is based on fluorescence images, other parameters could be quantified instead of the CW and viability (e.g., transformation efficiency, and gene expression). While the pipeline currently reports simple metrics (shape, size, and fluorescence intensity), the data acquired could be further refined using machine learning to classify and cluster cells or with deep-learning models to improve the accuracy of the analysis (i.e., by excluding signals coming from CW debris attached to a protoplast or predicting cell viability without the use of a binary threshold).

2.2 | Screening for Improved CW Recovery After Protoplasting Liquid-Grown Habituated Arabidopsis Cell Culture

We developed the Q-Warg workflow to solve the challenge we encountered when attempting to obtain "single plant cells" (SPC; isolated cells with recovered CW). Our aim was to obtain large populations of SPCs with relatively homogeneous size, recovered CWs, and no cell divisions, to establish them as a model system for plant CW and biophysical studies. Their largely spherical shape is ideal for physical and mechanical considerations and potential computational modeling approach. Such cells could then be used in studies of cell adhesion strength or CW mechanics. Our intention was to start with protoplasting and letting the cells recover their CW before using them. However, while many methods, publications, and protocols exist to promote CW recovery after protoplasting (Schirawski et al. 2000; Wu et al. 2009; Kuki, Higaki, et al. 2017; Pasternak, Paponov, et al. 2021; Jayachandran et al. 2023), none of the ones we tried yielded the expected results in our hands. Our preliminary observations led us to choose Arabidopsis-habituated root cell cultures (Pesquet, Korolev, et al. 2010; Ménard et al. 2017, 2024) as the starting material based on their apparent homogeneity. Similarly, our preliminary tests led us to use a modified protoplast extraction protocol (Yoo et al. 2007) and a modified regeneration medium (M; mannitol instead of trehalose (Kuki, Higaki, et al. 2017)) as the foundation for further optimization. Those preliminary protocol refinements, based on literature searches (Table S2), were assessed with qualitative observations of the protoplasts' shape and debris in the medium (issued from cell death). To go further and assess our progress methodically, we needed a quantitative way to compare the different conditions tested. Accordingly, we switched to developing and using our Q-Warg workflow.

24754455, 2025, 7, Downloaded from https://onlinelibrary.wiley.com/doi/10.1002/pld3.70090 by Umea University, Wiley Online Library on [21/07/2025]. See the Terms and Conditions (https://onlinelibrary.wiley.com/terms-and-conditions) on Wiley Online Library for rules of use; OA articles are governed by the applicable Creative Commons License

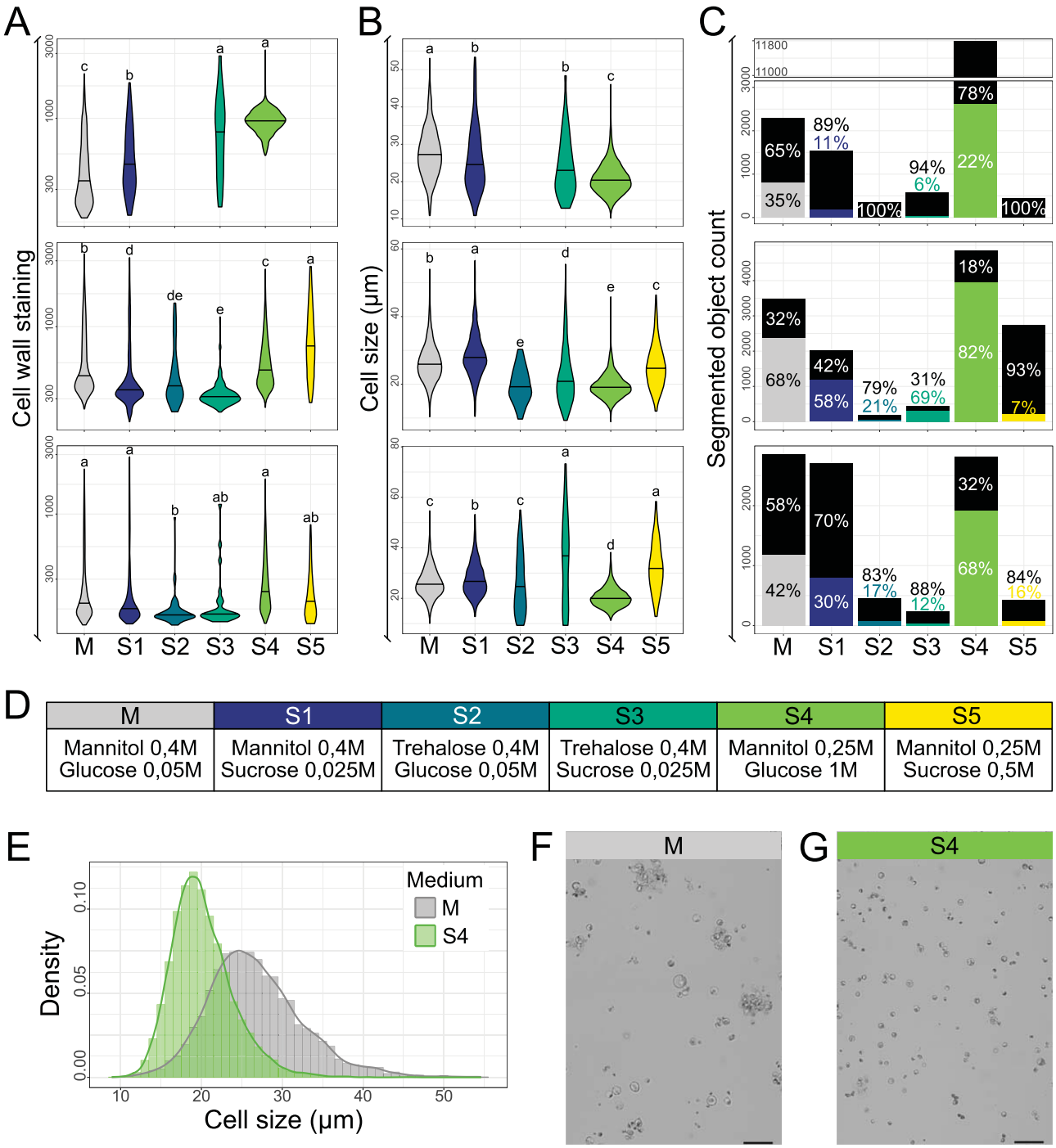

FIGURE 2 | Screening for the effect sugar composition in the medium to improve the CW recovery. (A–C) Plots from data processed with the Q-Warg pipeline on the effect of sugar composition in the medium for cell wall recovery, cell size, and viability, 4 days after protoplasting. Each plot corresponds to one replicate ($n = 3$). Note that in Replicate 1, no living cells was observed among the segmented objects; therefore, no quantification of CW staining intensity nor size is shown. (A) Cell wall mean intensity after staining with Calcofluor. (B) Cell size (diameter in µm). (C) Viability plots displaying the number of segmented objects (including debris, dead cells, or living cells). On violin plots, letters describe the statistically significant differences between populations determined by one-way ANOVA followed by Tuckey's HSD test ($p < 0,05$). In bar plots, each bar shows the total number of segmented objects and the proportion of objects negative for viability staining (in black) and living cells (in color). Chi-squared test of independence (significant if $p < 0.05$) was performed, followed by pairwise comparisons using the pairwise.prop.test function with Bonferroni correction for multiple testing. Results are in Data S1 (pages Fig 2_viability-stats). (D) Table with the tested media composition. All media contain Gamborg B5, MES, 1-µM NAA, and the corresponding sugars. (E) Cell size distribution for M and S4 media from the three replicates shown in B. (F–G) Four-day-old protoplast suspension in brightfield. Scale bar 100 µm. (F) Medium M, cells are forming aggregates. (G) Medium S4, cells are dispersed.

24754455, 2025, 7, Downloaded from https://onlinelibrary.wiley.com/doi/10.1002/pld3.70090 by Umea University, Wiley Online Library on [21/07/2025]. See the Terms and Conditions (https://onlinelibrary.wiley.com/terms-and-conditions) on Wiley Online Library for rules of use; OA articles are governed by the applicable Creative Commons License

From all parameters that were previously reported to have an impact on the protoplasting and the CW recovery (Tables S1 and S2), we decided to focus on two main aspects: sugars (Sx media; Figure 2) and hormones (Hx media; Figure S1). Sugars have two different roles: keeping the osmolarity of the medium (mannitol and trehalose; Kuki, Yokoyama, et al. 2020) and feeding the cells (glucose and sucrose). In the starting protocol, 1-naphthalene acetic acid (NAA) was used as an auxin source. We also tested the effect of 2,4-dichlorophenoxyacetic acid (2,4-D) and indole-3-acetic acid (IAA) on the CW recovery (Figure S1).

We found a high impact of the type of sugars used on the viability of the cells (Figure 2D). For the three replicates, Media S2, S3, and S5 showed a low number or no living cells. Both S2 and S3 contained trehalose instead of mannitol, which did not seem to help our cells recover their CW. Media S1 and S5 both contained sucrose and displayed either a low number of living cells and/or low CW staining intensity mean compared to the reference Medium M (Figure 2B). Interestingly, Medium S4 provided comparable results in CW staining as Medium M. Note, however, that the differences in apparent CW staining intensity could also be due to the differences in callose deposition rather than true CW recovery. Moreover, the number of living cells after 4 days in culture was higher. Additionally, the cells were, on average, smaller and more homogeneous in size than those in Medium M (Figure 2C,E). The smaller size may also explain why the cells in Medium S4 recover their CW more efficiently, as they need fewer CW components to be secreted by the cells to recover the CW. In addition to the quantitative data showing that Medium S4 was a good candidate, the cell suspension in Medium S4 showed well-isolated cells, while in Medium M, more clumps/aggregates were present.

The results of the auxin screening were less clear. In our hands, the source of auxin did not seem to have any major impact on the CW recovery at the concentrations we tested when using our base medium (Figure S1B). Nevertheless, Medium H1 seemed to promote CW recovery a bit more than Medium M, suggesting that using a higher concentration of NAA could help the protoplasts recover their CW. Zhang et al. (2024) showed that a higher concentration of auxin enhanced the CW recovery. We then screened several concentrations of NAA (0–30 μM and 5-μM increment), this time using Medium S4 as base, to check if we could further increase CW recovery in our medium (Figure S1E). For both 5 and 10 μM, a significant increase in CW recovery was observed. As the proportion of living cells was higher with 5 μM of NAA, we chose to work with this concentration (Figure S1E).

Ultimately, with this approach using the Q-Warg pipeline, we successfully improved our medium for CW recovery on the protoplasts extracted from Arabidopsis-habituated root cell culture maintained at Umeå Plant Science Center (UPSC). Starting with the Medium M, we found that the Medium S4 led to a 1.61- to 3.22-fold increase in the total number of living cells, up to a 2.12-fold increase in CW staining mean intensity, and more homogeneous cell sizes (from 26.7 ± 5.89 μm for M to 20.1 ± 3.82 μm for S4). Note that the size variability might be partially reduced because of the higher osmotic pressure exerted on the cells in Medium S4. Building on Medium S4, increasing the NAA concentration from 1 to 5 μM resulted in a 1.12-fold increase in the total number of living cells and a 1.08-fold increase in cell wall staining mean intensity, while cell size and homogeneity remained similar (from 19.9 ± 4.71 to 19.1 ± 3.92 μm). With this, we propose an improved medium for our use case, based on Medium S4 and containing 5-μM NAA that we name CRRUM (CW recovery root cells UPSC medium).

Note that we performed the original sugar and hormone screen with three independent biological replicates to assess the robustness of the pipeline as a screening approach. The three biological replicates, while showing some differences, are largely in accordance with each other. We thus believe that our workflow can also be used as a robust and high-throughput screening tool by first testing various media and conditions and then using replicates for a subset of more promising media to confirm and refine choices in medium optimization.

2.3 | Further Selection of Single Plant Cells With Recovered CWs

Despite our efforts to improve CW recovery under our lab conditions, we have yet to identify a medium that reproducibly enables close to 100% of the cells to fully recover their CW. Furthermore, with the Q-Warg pipeline, we quantify fluorescent signal from CW staining, which highlights the wide disparity in CW recovery. There is no clear bimodal distribution of cells with and without recovered CWs. Not all cells seem to recover their wall at the same pace. This raises the following question: At which point do we consider the CW as "recovered"? Furthermore, while our workflow effectively characterizes these properties, it does not allow the selection of cells with recovered walls for further use.

One possibility to overcome this limitation is to sort cells with FACS based on cell size and fluorescence staining intensity. Before sorting, the cell suspension was stained for viability and CW recovery assessment. The sorted cell suspension contained only isolated cells that were positive for both viability and CW staining (Figure S2). However, during sorting, the cells are exposed to high pressure and friction forces, which may be harmful and could reduce yield. This method is suitable if a large population of cells meets the sorting requirements and the loss of some cells does not significantly affect the outcomes. Using FACS also implies the availability of suitable equipment, ideally sorting to be done in sterile conditions, and requires specific skills that may not be widely accessible in many plant biology labs.

One key function of the CW is to balance turgor pressure coming from the cytoplasm. After CW removal, protoplasts are initially kept in an iso-osmotic medium to avoid bursting before the CW is recovered. In turn, it can be argued that a non-biased binary (yes/no) estimation of CW recovery would be whether or not a cell can sustain its own turgor pressure when it is placed back in pure water or in the normal cell culture growth medium (Figure 3C). A sudden change of medium osmolarity could both provide a binary estimate of CW recovery when tested through our quantitative workflow and serve as a

24754455, 2025, 7, Downloaded from https://onlinelibrary.wiley.com/doi/10.1002/pld3.70090 by Umea University, Wiley Online Library on [21/07/2025]. See the Terms and Conditions (https://onlinelibrary.wiley.com/terms-and-conditions) on Wiley Online Library for rules of use; OA articles are governed by the applicable Creative Commons License

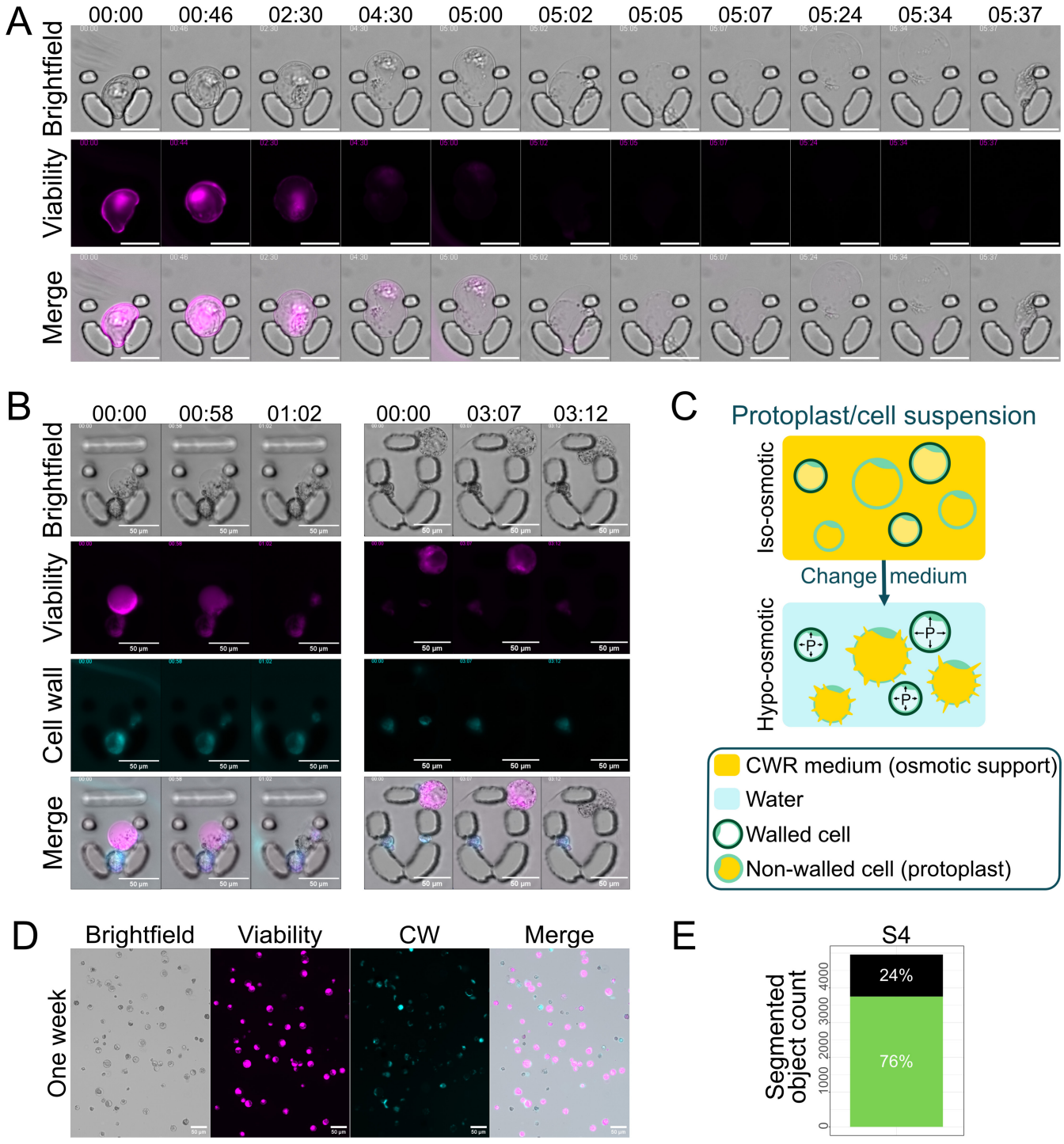

FIGURE 3 | Cell selection based on osmolarity differences in culture medium and single plant cells. (A,B) Osmotic shock performed on SPC 4 days after protoplasting. MilliQ water is flowing inside the chip from Time 0. The change in osmolarity makes the cells inflate and burst. The viability signal shows that the cell was alive at the start of the experiment. Note that the decrease in signal does not entirely correspond to the death of the cell as FDA stays fluorescent after conversion by cellular enzymes. In this case, the decrease of the signal is partially due to the bleaching of fluorescence. Complete movies in Videos S1–S3. (A) Opened trap. (B) Closed traps. Cell walls were stained with Calcofluor. (C) Scheme representing the osmotic shock strategy: The protoplast culture contains both walled and nonwalled cells. The nonwalled cells (protoplasts) are more susceptible to changes in medium osmolarity. In a hypo-osmotic medium, only walled cells will survive. (D) Single plant cells cultured into Medium S4 for 1 week. Cells are stained with FDA for viability and Calcofluor for CW. Imaged in microfluidic taped channels. (E) Quantification of living cells after 1 week of culture in S4.

means to eliminate (burst) cells with nonrecovered CW from a population. As a proof of concept, we first exposed the cell suspension (4 days after protoplasting in Medium S4) to pure water. To monitor the effect on individual cells, we used a microfluidic chip containing U-shaped traps (Sakai et al. 2019). This allowed us to keep the cells trapped in a fixed field of

24754455, 2025, 7, Downloaded from https://onlinelibrary.wiley.com/doi/10.1002/pld3.70090 by Umea University, Wiley Online Library on [21/07/2025]. See the Terms and Conditions (https://onlinelibrary.wiley.com/terms-and-conditions) on Wiley Online Library for rules of use; OA articles are governed by the applicable Creative Commons License

view for live imaging while allowing a dynamic change of the liquid medium. Switching from Medium S4 to pure water led most of the observed cells to inflate and burst within a few minutes (Figure 3A,B). Observations using both viability and CW staining (Figure 3B) further suggest that cells with a qualitatively well-recovered wall (clear fluorescent signal) do not burst upon change of medium while protoplasts that do not appear to have CW staining burst. It is also likely that smaller walled cells showed a stronger resistance to the osmotic shock as a similar increase in turgor pressure would lead to higher stress in the CW of larger cells (Sapala et al. 2018; Figure 3B). These preliminary observations indicate that our hypo-osmotic shock approach could be useful at a larger scale. We then turned to look at the effect on large-scale cell populations and characterized the effect with the Q-Warg workflow. Pure water appeared to be too much of an osmotic shock, which may even lead to bursting of walled cells (Figure 3A,B). We used two media that contained less osmotic support than extraction or cultivation media for protoplasts to perform the osmotic shock: CRRUM without mannitol (CRRUM-noM) and the initial cell culture medium MS 3%. The cells were transferred after 4 days in culture in CRRUM into their new medium. Quickly all the cells in MS 3% died, suggesting that this medium transition had a negative effect on cell survival regardless of their CW recovery status (Figure S3C). In CRRUM-noM, we observed a quick inflation of the cells that can be attributed to the decreased osmotic pressure (Figure S3A). There was also a strong reduction in the number of cell-like objects counted and in the percentage of objects considered as living cells. Surprisingly, while we could expect the remaining living cells to be primarily strongly stained for CW, our quantification revealed the opposite trend, with cells having on average lower CW staining than the cell population kept in medium with osmotic support (Figure S3B). However, the comparison of CW staining intensity should be made carefully as the difference in medium osmolarity could affect staining capacity. Furthermore, apparently bright cell wall staining as reported by Calcofluor staining could also result from callose deposition. Thus, they may not correlate with properly regenerated cell walls displaying mechanical integrity able to sustain turgor pressure. Interestingly, after the osmotic shock, the CW fluorescence intensity average signal increased over cultivation time (3 days) while this trend is not seen in the medium with maintained osmotic support (Figure S3C). This could suggest that the remaining cells with mild cell wall signal, increasing over time, were those with "true" cell wall regeneration rather than bright callose patches. Thus, while in the current experiment we did not obtain the expected effect of binary selection of cells with recovered walls, the osmotic shock approach could still be a promising approach to select cells undergoing proper cell wall regeneration (Seyama and Kondo 2012). Furthermore, because we see an increasing trend in average cell wall staining after osmotic shock but not when cells are kept in the same medium, our results suggest that this approach may have the added benefit of further promoting CW recovery over time as suggested in other methods (Sakai et al. 2019). Note however that another explanation could be that the increased turgor pressure in the remaining living cells after the osmotic shock induces a stress response leading to the increased secretion of callose rather than cellulose.

2.4 | Assessment of Isolated Cell Viability

To assess the behavior and viability of SPCs over a long time, we used a small 3D printed microscope: Openflexure (Collins et al. 2020). Cells were plated on a glass-bottom Petri dish with a poly-lysine coating to maintain them in place. Using this DIY setup, the cells were maintained and imaged every 15 min for about 5 days. We could observe movement inside the cytoplasm of the cells, showing that they were still alive (Movie S1). In parallel, cells were kept in S4 for a week in the dark, after which they were stained to assess their viability and cell wall recovery. Notably, 74% of the segmented objects were computed as living cells (positive FDA signal and high circularity index), indicating that they could survive for a long time as single cells (Figure 3D,E). Interestingly, cells did not seem to divide in both setups, which gives us a large time window to use SPC in further experiments. To pursue divisions and calli development, cells might require other nutrients and/or hormones.

2.5 | Screening for CW Recovery in Media Aimed to Enhance Cell Division

First, to test the reusability of the Q-Warg pipeline, a trial run has been conducted in other hands in a different lab with different biological materials: at the Laboratory of Biochemistry, Wageningen University, using PSB-D cell culture derived from stem explants of *Arabidopsis thaliana* Landsberg erecta (Ler) ecotype. Unlike the previous results, imaging was done with a confocal microscope, showing the adaptability of the pipeline. We first conducted a similar screening of NAA concentration (ranging from 0 to 4 μM) within the initial Medium M during the first days of culture after protoplasting to assess cell viability. We could observe that in the absence of NAA, less than 30% of the segmented objects were living cells after 2 days of culture. By increasing the NAA concentration, we could note a positive effect on cell viability. After 2 days of culture, the more NAA was present in the medium, the larger the viable proportion of cells was (Figures 4A and S4). We also checked whether the CW recovery was increased at higher NAA concentrations, yet in those conditions, we could not observe a significant difference in CW recovery (Figure S4A).

In light of these results, we initiated a medium screening to determine the requirements for promoting micro-calli formation after protoplasting. Because cell divisions can only occur once the CW has been recovered, the first goal was to establish which parameters maintain a high viability and, second, promote CW recovery but using base media that contain hormones and nutrients aimed at enhancing cell division and regeneration. The screening was performed with three media over 3 days starting on the day of the protoplast extraction. In two tested media, "Murashige and Skoog with Minimal Organics" (MSMO) and "Protoplast Regeneration Medium" (PRM; Chupeau et al. 2013), kinetin, a form of cytokinin, was used to promote cell division when associated with auxin (respectively NAA or 2,4-D; Barciszewski et al. 2007). To compare with the previous results obtained with the root cell culture used in the beginning of this study, we also tested Medium M. Over this period of observation, we did not notice a significantly better medium for CW recovery.

24754455, 2025, 7, Downloaded from https://onlinelibrary.wiley.com/doi/10.1002/pld3.70090 by Umea University, Wiley Online Library on [21/07/2025]. See the Terms and Conditions (https://onlinelibrary.wiley.com/terms-and-conditions) on Wiley Online Library for rules of use; OA articles are governed by the applicable Creative Commons License

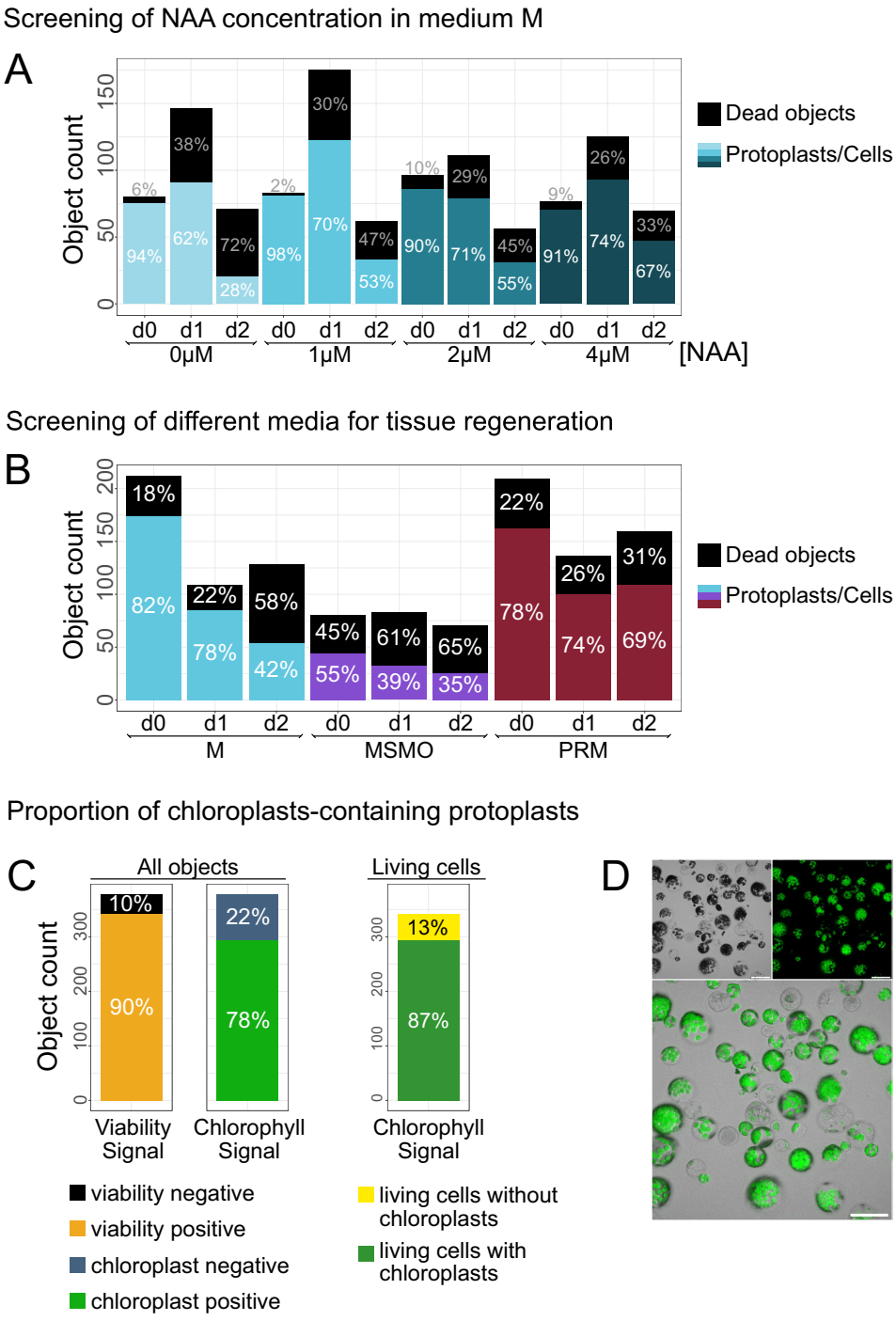

FIGURE 4 | Challenging the Q-Warg pipeline. (A) Viability plot for NAA concentration screening in Medium M. Four different concentrations of NAA have been tested. d0 corresponds to the protoplasting day. (B) Viability plot for medium screening. Three media for tissue regeneration were tested. d0 corresponds to the protoplasting day. (C,D) Protoplast extracted from *Arabidopsis thaliana* seedlings and imaged the day of extraction. (C) Left bar plot represents the proportion of living cells in yellow (90%). The middle bar shows the proportion of autofluorescent objects based on chlorophyll autofluorescence (78%). The right bar shows the proportion of chloroplast-containing cells among the living cells. (D) Protoplast suspension in brightfield (top left), autofluorescence of chlorophyll (top right), and merged image (bottom). Scale bar 50 µm. In plots, object count corresponds to the number of segmented objects (including debris, dead cells, or living cells). Each bar shows the total number of segmented objects and the proportion of objects negative for viability staining (in black) and living cells (in color). Protoplasts are issued from PSB-D cell culture. Chi-squared test of independence (significant if $p < 0.05$) was performed, followed by pairwise comparisons using the pairwise.prop.test function with Bonferroni correction for multiple testing. Results are in Data S1 (pages Fig 4_viability-stats).

24754455, 2025, 7, Downloaded from https://onlinelibrary.wiley.com/doi/10.1002/pld3.70090 by Umea University, Wiley Online Library on [21/07/2025]. See the Terms and Conditions (https://onlinelibrary.wiley.com/terms-and-conditions) on Wiley Online Library for rules of use; OA articles are governed by the applicable Creative Commons License

Cells in M and MSMO showed a similar increase in CW signal, but viability decreased to about 40% of the segmented objects (Figure 4B). PRM medium did not show an improved CW recovery compared with M and MSMO (Figure S4B). However, the proportion of living cells after 2 days was maintained at 70% of the segmented objects, which made this medium promising. Future work will determine the best condition to achieve quick cell divisions to reach the micro-calli stage.

2.6 | Pipeline Versatility: Quantification of Chloroplast-Containing Cells

The Q-Warg pipeline is based on brightfield and fluorescence imaging and quantification and is not limited to viability and CW staining. The intensity quantification can in principle be done on any fluorescence marker or autofluorescence signal. To show the versatility of the pipeline, we quantified the proportion of chloroplast-containing protoplasts extracted from whole seedlings. Using the viability proportion plot, we first quantified the proportion of living cells in the suspension with the viability staining (FDA). Then inside this population of living cells, we used the workflow to quantify the number of cells containing chloroplasts (Figure 4C,D). To do this, instead of taking the fluorescence coming from a viability staining as input, we used the autofluorescence of chloroplasts. The plot given by the pipeline is then used to report the cells or objects with chloroplasts versus those without, based on their autofluorescence. In this experiment, among the objects segmented by the pipeline, 90% were viable protoplasts, and 78% presented an autofluorescence signal from chloroplasts. Using these data and the unique IDs of cells analyzed through the pipeline, we then calculated that 87% of the living cells extracted from those seedlings contain chloroplasts (Figure 4C "Living cells").

3 | Conclusion and Perspectives

In this work, we introduced the Q-Warg pipeline, an imaging and image processing-based workflow aimed at making studies of protoplast culture, viability, and CW recovery more accessible, quantitative, and standardized. We further applied it in several use cases to show its usefulness in different configurations, demonstrating its robustness and versatility.

Our initial aim when developing this pipeline was to create a tool that we could confidently use to assess our progresses when optimizing CW recovery media for the obtention of "single plants cells." Thus, in this work, we report the steps taken in this direction by testing the quantitative effect of changing a subset of the CW recovery medium composition, namely, the sugars and auxins used, and finding an improved medium. However, given the number of parameters that may influence protoplast culture and CW recovery (Table S1) and the range of possible values to be tested for each parameter, there is a virtually infinite number of media combinations to be tested. This is obviously impossible for practical reasons, but it is in principle possible to use design of experiment approaches to explore parameter spaces and define optimal settings without having to test every possible combination (Cano et al. 2012; Peng et al. 2022). We also believe that our workflow could further help in the future to streamline the media optimization process. The standardized nature of the pipeline also aimed to increase the reusability of the data. We provide a detailed user guide for the whole procedure (Method S2) and aimed to make the computational workflow user-friendly. We also strongly encourage future users to deposit their data in publicly accessible repository for future reuse. In practice, during the medium optimization process, it is more reasonable to test a restricted set of parameters, until reaching an acceptable result and moving on. Researchers have been doing this for several decades, but unfortunately those optimization steps are rarely reported, nor quantitatively measured, and there is no standardized format available. Instead, in vitro culture medium optimization is almost referred to as an art, only mastered by a few experts with decades of experience. We believe that the instinctive expertise acquired by such experts could be understood scientifically and be made available more broadly if we can generate enough standardized data on protoplast viability and regeneration and study them through advanced multivariate analyses or novel deep learning approaches. We could, for instance, imagine training a model with a large dataset gathering matching information on the parameters used in the media, types of tissues, varieties, species, growth conditions, and so on and matching quantification of viability and CW recovery. In turn, we may be able to interrogate the model to predict a set of media to test for further optimization, given a species, variety, tissues, and growth conditions of choice. This would effectively allow a much shorter time for medium refinement, by using complex knowledge from prior optimization experiments as a starting point for a subset of media to test. In parallel, the Q-Warg pipeline could be used for quantitative screening of large sets of mutants with improved or impaired protoplast viability or CW recovery to decipher the biological mechanisms regulating these processes.

The pipeline we developed here is also potentially highly versatile. Because of our original aim, we focused mainly on cell viability and CW recovery after protoplasting. However, the pipeline can also be used to explore other parameters. Here, we also used it to determine the percentage of chloroplast-containing cells inside a population of protoplasts extracted from seedlings. This workflow could also be used to check transformation efficiency with a fluorescent reporter or other parameters that can be observed quantitatively with fluorescent dyes or reporters at the cell level.

Encouraging open data practices and leveraging deep learning approaches, thanks to datasets acquired with such tools, could help make significant strides in unraveling the biological complexity of protoplasts, ultimately contributing to more robust and reproducible research outcomes and biotechnological applications.

4 | Methods

4.1 | Biological Material

4.1.1 | Root Cell Culture

The cell culture used in this study (unless stated otherwise) is derived from the root cells of *A. thaliana*, ecotype Colombia, and was previously reported (Pesquet, Korolev, et al. 2010). This cell

24754455, 2025, 7, Downloaded from https://onlinelibrary.wiley.com/doi/10.1002/pld3.70090 by Umea University, Wiley Online Library on [21/07/2025]. See the Terms and Conditions (https://onlinelibrary.wiley.com/terms-and-conditions) on Wiley Online Library for rules of use; OA articles are governed by the applicable Creative Commons License

culture was habituated via prolonged culturing with decreasing exogenous hormones until it became able to grow and divide without exogenous hormones.

Prior to our set of experiments, the cell culture was re-screened for habituation (Ménard et al. 2017, 2024). Calli were grown on 1% plant agar (Duchefa) growth medium plates. One callus was used to start the new cell suspension to have a clonal culture. Growth medium MS 3% contains Murashige and Skoog medium including vitamins (M0222, Duchefa), 3% sucrose (VWR), and MES 20 mM. The pH is adjusted to 5.7 with KOH. Cells are growing in the dark under constant shaking (22°C and 120 rpm). The cell culture was maintained weekly by inoculating 72 mL of fresh MS 3% with 8 mL from the 1-week-old culture.

4.1.2 | PSB-D Culture

A. thaliana, ecotype Landsberg, cell suspension cultures (PSB-D) were donated by Geert de Jaeger (ABRC stock no. CCL84840) (Menges and Murray 2002; Van Leene et al. 2011). MSMO contains Murashige and Skoog Basal Salts with minimal organics 0.44% (Sigma-Aldrich) and sucrose 88 mM. The pH is adjusted to 5.7 with KOH. After autoclaving, 2.7-μM NAA and 0.23-μM kinetin were added. PSB-D cultures were grown in 50-mL MSMO (dark, 25°C, and 135 rpm) and were maintained weekly by taking 2.5 mL from the 1-week-old culture with 47.5 mL of fresh MSMO.

4.1.3 | Seedling Growth

A. thaliana, ecotype Columbia-0 (Col-0), seeds were sterilized by washing them with 70% ethanol, followed by a treatment with 0.8% NaOCl for 3 min. Seeds were washed five times with ultrapure water and were kept in water in the dark at 4°C for 2 days. Seeds were then sown on MS agar plates. MS agar plates contain half-strength Murashige and Skoog medium (Duchefa), 5-mM MES, and 0.8% plant agar (Duchefa). The pH was adjusted to 5.7 with KOH. The plates were vertically incubated at 22°C under a long day growth period (16-h light and 8-h dark).

4.2 | Protoplast Extraction

4.2.1 | Root Cell Culture

The protocol was adapted from Yoo et al. (2007) and is detailed in the protocol (Method S1). In brief, cells are incubated in an enzymatic solution for 4 h in the dark at 120 rpm and 24°C in nontreated six-well plates. Enzymatic digestion is stopped with W5, and the protoplast suspension is filtered through a 70-μm nylon basket before centrifugation and resuspension in culture medium. For all root cell culture protoplast extractions, the cell culture was 4 days old (4 days after refreshing medium).

4.2.2 | PSB-D Protoplast Extraction

PSB-D protoplasts are extracted similarly to root cell culture protoplasts, with the following adjustments. A 5-day-old PSB-D culture was used. The culture was incubated in the dark at 200 rpm and 25°C. Protoplasts were filtered through a 40-μm nylon basket. The final pellet was resuspended in 1 mL of the desired medium. Protoplast density was adjusted to $5.0*10^4$ cells/mL, and 200 μL of suspension was transferred to each well of an Ibidi μ-Slide (eight-well high, polymer coverslip, and uncoated). Slides were placed in a dark growth chamber at 22°C for 3 days.

4.2.3 | Seedling Protoplast Extraction

The protocol is detailed in Method S1. The protocol is adapted from Zhai et al. (2009) for protoplast extraction of 18-day-old seedlings with the following modifications. The protoplast suspension was filtered through a 40-μm nylon basket. W5+ was used instead of W5 to retrieve protoplasts within the sucrose gradient. W5+ differs from W5 by a higher KCl concentration (11 mM instead of 5 mM) and the inclusion of glucose (5.6 mM). Protoplast density was adjusted to $5.0*10^4$ cells/mL, and 200 μL of suspension was transferred to each well of an Ibidi μ-Slide (eight-well high, polymer coverslip, and uncoated). Seedling protoplasts were imaged directly after extraction.

4.3 | CW Recovery Medium

Initial medium for CW recovery, Medium M, contains Gamborg B5 (Gamborg's B-5 Basal Medium with minimal organics, G5893, Sigma-Aldrich), 0.4-M mannitol, 0.05-M glucose, 1-μM NAA, 20-mM MES filled up to the wanted volume with MilliQ water, and pH 5.7 adjusted with KOH. The different combinations of sugars and hormones that have been tested are reported in Figure 2A. The protoplasts were transferred directly after extraction in medium for CW recovery and kept in the dark at 22°C without shaking. After screening, the medium CRRUM was used for CW recovery with root cell culture: S4 with 5-μM NAA. For all changes of medium, the cell suspension was placed in Falcon 50-mL tubes and centrifuged at 200 g in a swing-rotor centrifuge for 3 min at room temperature. The supernatant was carefully removed by pipetting, and the new medium was added. Cells were resuspended by gently turning over the Falcon tube. The media used for CW recovery with the PSB-D cells were CRRUM, MSMO (previously described), and protoplast regeneration medium (PRM). PRM was modified from Chupeau et al. (2013) and contains half-strength Murashige and Skoog medium (Duchefa), 20-mM MES, 0.3-M mannitol, 0.2-M glucose, 4.5-μM 2,4-D, 0.46-μM kinetin filled up to the wanted volume with MilliQ water, and pH 5.7 adjusted with KOH.

4.4 | Microscopy Sample Preparation and Imaging

4.4.1 | Protoplasts Derived From Root Cell Culture

Viability was assessed by FDA (F1303 Thermofischer). Four minutes before imaging, FDA was added to the cell suspension to reach 8 μg/mL. For CW characterization, the cells were stained just before imaging with Calcofluor White (Calcofluor White Stain, Sigma-Aldrich) diluted 1:100 directly in the cell suspension. Double-stained cells were then loaded in an Ibidi channel chamber (μ-Slide VI 0.4 Bioinert) or an in-house

24754455, 2025, 7, Downloaded from https://onlinelibrary.wiley.com/doi/10.1002/pld3.70090 by Umea University, Wiley Online Library on [21/07/2025]. See the Terms and Conditions (https://onlinelibrary.wiley.com/terms-and-conditions) on Wiley Online Library for rules of use; OA articles are governed by the applicable Creative Commons License

chamber. In-house chambers are composed of a microscopy slide on which strips of microfluidic tape (S5005DC, Adhesive Applications) are put to form channels and maintain a distance from the coverslip (see protocol file Method S1). Fluorescence imaging was done with a Leica DMi8 inverted brightfield and epifluorescence microscope with a motorized stage and navigator function. The microscope is equipped with a 10× objective lens (NA 0.32, air objective) and a Leica DFC9000GT camera mounted on a 1× C-mount adapter. Tile images made of 3 × 9 (27) individual images (12bits, 2048 × 2048 resolution for each image, and pixel size of 1.048 × 1.048 μm) were acquired with the Navigator function of the microscope using a 10% overlap. Tile images were merged with the LAS X software (Leica Microsystems, Germany). Before acquisition, autofocus is done on the brightfield channel. Three channels were acquired: brightfield, FDA signal excited with 460-nm LED, and emission detected above 515 nm (long pass filter) and Calcofluor signal excited with 365-nm LED and emission detected between 435 and 485 nm. The same procedure was used to quantify viability and CW recovery following osmotic shock (Figure S3).

4.4.2 | Protoplasts Derived From PSB-D and Seedlings

Protoplasts were imaged in Ibidi μ-Slide (eight-well high, polymer coverslip, and uncoated) with an inverted Nikon ECLIPSE Ti2 microscope equipped with a Nikon C2 confocal laser scanning head and a 40× (NA 0.95) dry objective. Five minutes before imaging, protoplasts were stained with 5-μg/mL FDA. PSB-D protoplasts were also stained with Calcofluor White (Calcofluor White Stain, Sigma-Aldrich) diluted 1:100. Calcofluor White/chloroplasts and FDA were excited sequentially using a 405- and 488-nm laser line, respectively. Calcofluor White/chloroplast fluorescence was detected using a dual-bandpass filter (C2 Filter Cube DAPI/Cy5 Dual, MHE46660) between 440 and 460 nm (Calcofluor White) and 680 and 720 nm (chloroplasts), and FDA fluorescence was detected between 500 and 550 nm (C2 Filter Cube 525/50595/40, MHE46770). With the 488-nm laser line, transmitted light was also collected. Z-stacks (512 × 512 pixels, pixel size 0.62 μm) were taken at 1-μm intervals of the bottom 12 μm of the cells. For Q-Warg analysis, maximum-intensity Z-projections were used for the fluorescence channels. For CellPose segmentation, we used the topmost plane of each z-stack, which corresponds approximately to a cross-sectional image of the middle of each cell.

4.5 | Computational Workflow

The analysis workflow is first based on (1) cell segmentation on the brightfield image using CellPose, (2) an ImageJ macro to extract quantitative information from the images, and (3) an R script to analyze and represent the quantitative data. The procedure described here can be downloaded from GitHub (https://github.com/VergerLab/Q-Warg) and Methods S3 and S4. The overall concept and procedure are described in the main text (Figure 1), and a detailed step-by-step description of the procedure is available in the user guide available in the GitHub repository and as Method S2.

4.5.1 | Cell Segmentation

Cell segmentation is done on the brightfield image with the generalist model cyto3 (Stringer and Pachitariu 2025). Used settings were default except for the cell diameter (40 pixels) and the flow threshold (0.2). The label image generated from the segmentation was saved as PNG. Details on how to use CellPose can be found in the Q-Warg user guide (Method S1).

4.5.2 | Quantification

We developed a batch processing ImageJ macro using Fiji (Schindelin et al. 2012) to extract quantitative information from segmented label images and the corresponding cell wall and viability fluorescence images (CWRegenerationQuantification.ijm; Method S3). The macro splits the multichannel image (brightfield, CW, and viability) and saves individual images as tif as well as brightfield images with cell segmentation (contours) overlap. The macro uses the ImageJ plugin MorpholibJ (Legland et al. 2016) to extract morphometric information (*Plugins>MorphoLibJ>Analyze>Analyze Regions*) on individual cells from the label image, as well as fluorescence intensity (*Plugins>MorphoLibJ>Analyze>Intensity Measurements 2D/3D*) on the CW and viability images for individual cells using the label image.

4.5.3 | Data Analysis

We developed an R script in a markdown notebook (QWARG.Rmd; Method S4) usable in RStudio (https://posit.co/download/rstudio-desktop/) to analyze the data issued from the quantification. Data tables generated by the CWRegenerationQuantification.ijm (additional File 4) macro were combined and organized to be treated all at once (tidyverse; Wickham et al. 2019). Automatic thresholding was computed to discriminate dead and living cells using the autothreshold library (Nolan et al. 2023) and applied in a shiny app using plotly to render interactive plots (shiny; Chang et al. 2024; Create Interactive Web Graphics via "plotly.js" [R package plotly version 4.10.4] 2024). The plots were done with the ggplot2 library. Another Shiny app helps check the results of the thresholding and cell segmentation by linking interactive plots (plotly) to the microscopy images (magick; Ooms 2024). All information about other libraries used can be found in the user guide (Method S2).

4.5.4 | Statistical Analysis

We performed statistical analysis within the R notebook using the agricolae library (de Mendiburu 2023). One-way analysis of variance (ANOVA) followed by Tukey's honestly significant difference (HSD) test was performed for multiple comparisons of means for CW staining intensity and cell size plots. Chi-squared test of independence (significant if $p < 0.05$) was performed, followed by pairwise comparisons using the pairwise.prop.test function with Bonferroni correction for multiple testing.

24754455, 2025, 7, Downloaded from https://onlinelibrary.wiley.com/doi/10.1002/pld3.70090 by Umea University, Wiley Online Library on [21/07/2025]. See the Terms and Conditions (https://onlinelibrary.wiley.com/terms-and-conditions) on Wiley Online Library for rules of use; OA articles are governed by the applicable Creative Commons License

4.6 | Osmotic Shock in Microfluidic Chips

4.6.1 | Chip Fabrication

The microfluidic chips were fabricated according to the method detailed in Sakai et al. (2019). Starting from a SU8-on-silicon master mold (IPGG, Paris), a 9:1 PDMS (Silgard 184 Silicone Elastomer, Dow) mixture is poured on top of it, degassed for 2 hours in a vacuum chamber, and cured at 70°C overnight. The chips are then individually cut with a razor blade, and inlets and outlets are created using a biopsy puncher (1-mm diameter, pfm medical). PDMS chips are then rinsed with isopropanol and stuck to a glass bottom petri dish (WPI Fluorodish P35-100) in a cleanroom (Nanolab, Umeå) using an oxygen plasma cleaner (Plasma cleaning system ATTO, 0.35 mbar, 36 s).

4.6.2 | Chip Preparation

Before loading the cells, a flow of 96% EtOH was performed not only to sterilize the tubing (0.022 "ID × 0.042" OD, PTFE, Masterflex) and the chip but also to reduce the apparition of bubbles in the setup. Then, a filtered (0.2-μm filter) of pluronic F-127 0.02% solution in water was added overnight inside the chip. The pluronic solution was replaced with medium before loading the cells.

4.6.3 | Osmotic Shock

Four days post-extraction, the cell suspension was stained as explained previously with Calcofluor and FDA. The cells were loaded at 100 μL/min with a DIY syringe pump (Baas and Saggiomo 2021) until most of the traps contained a cell. MilliQ water was then pumped into the chip at 50 μL/min. Short-term brightfield timelapses of the chip are recorded with the Leica Dmi8 microscope.

4.6.4 | Timelapse Experiment

Protoplasts were cultured in FluoroDish (FD35, World Precision Instruments) coated with poly-lysine to maintain cells in place. FluoroDish glass bottom was covered by a solution of poly-L-lysine 0.1% (P8920, Sigma-Aldrich) for 5 min at room temperature. The liquid was removed as much as possible with a pipette and quickly dried with an air gun. The plates were dried in an oven at 60°C for 1 h. A 3D printed microscope Openflexure (high resolution version, Collins et al. 2020) was used to image the culture in brightfield, without staining. Images were taken every 15 min with white LED illumination for the duration of the experiments. Cells were cultured at room temperature (20°C–22°C).

4.7 | Fluorescence-Activated Cell Sorting

Before analysis and sorting, the cells were washed from the culture medium and put into W5 modified (W5m). The cell suspension was transferred into a 15-mL Falcon tube and centrifuged at 200rcf (swing out rotor centrifuge) for 5 min, RT. W5m contains only 2-mM calcium (instead of 125 mM) to avoid the precipitation with the sheath fluid (70% FACS Flow; BD Bioscience, San Jose, CA, USA) used during sorting and 0.1% BSA to prevent sticking of the cells to the plastic walls of the sorting plate.

The FACS BD Aria III equipped with four lasers: violet (405 nm), blue (488 nm), yellow green (561 nm), and red (633 nm) lasers (BD Biosciences, San Jose, CA, USA). BD FACSDiva software Version 7.0 was used for handling the cytometer and respective data analysis. For each condition, the nonstained sample was subjected to analysis as a negative control. Cell suspension was stained for 30 min with a 1:1000 dilution of CarboTrace 680 for CW staining and FDA (5-mg/mL stock solution, predilution: 1.6 μL for 1-mL medium, then add 1.6 μL of the predilution for 1-mL cell suspension).

Protoplast analysis and sorting: Filtered protoplast suspension through 70-μm Flowmi Cell strainer (SP Bel-Art, Wayne, NJ, USA) was loaded in the cell sorter (room temperature, mild agitation of 100 rpm) and forced through the cuvette in a single-file stream, where laser lights intercepted the stream at the sample interrogation point. After passing through the cuvette, the stream entered the integrated 100-μm nozzle tip, where the drop drive broke the stream into the droplets for sorting. The forward scatter (FSC) of light was initially filtered through a 1.5 neutral density filter and then perceived by a photodiode detector with a 488/10 bandpass filter. Light scatter information was collected to identify the protoplast population and to design sorting strategy (Figure S2).

Different protoplast populations based on fluorescent properties given by used fluorophores were sorted for microscopy analysis into 500 μL of CWR medium in a 24-well plate. To remove the debris, all events smaller than 16 μm were disregarded. The cells were sorted based on their viability (FDA staining) and their CW staining (CarboTrace 680). We used CarboTrace 680 instead of Calcofluor for CW staining to limit the toxicity applied to the cells. To identify and subsequently exclude doublets (the droplets containing more than one protoplast), the ratio of fluorescence signal width to the respective area was measured (Suda et al. 2007).

Author Contributions

The authors take full responsibility for this article.

Acknowledgments

We thank Åsa Strand and Xu Jin for providing the root cell culture material and initial technical help. We thank Adrien Heymans for helping with the statistical part of the R script. We thank Pauline Durand and Cyril Grandjean, Antoine Chevallier and Isaty Melogno, and Mateusz Majda and Lukas Hoermayer for the discussions about protoplast extraction and culture optimization. We thank Remko Offringa and Loïc Talide for giving us feedback on the manuscript. We thank the facilities and technical assistance of the Umeå Plant Science Center (UPSC), the microscopy facility, and the growth facility. We thank the NanoLab (Physics Department, Umeå University) for the technical resources for microfluidic chips fabrication. This work benefited from the technical contribution of the joint service unit CNRS UAR 3750 (Paris, France) at IPGG. This work was supported by grants from the Swedish Research Council (VR, 2020-03974), Novo Nordisk Foundation (NNF21OC0067282), Åforsk Foundation (20-502), Knut and Alice Wallenberg Foundation (KAW 2022.0029) to S.V. R.F. is financially supported by the TopSector TKI Horticulture and Starting Materials, the Netherlands, through the

24754455, 2025, 7, Downloaded from https://onlinelibrary.wiley.com/doi/10.1002/pld3.70090 by Umea University, Wiley Online Library on [21/07/2025]. See the Terms and Conditions (https://onlinelibrary.wiley.com/terms-and-conditions) on Wiley Online Library for rules of use; OA articles are governed by the applicable Creative Commons License

project TU202312. J.S. and P.S. are funded by the European Research Council project Catch, project number 101000981. I.A. and V.S. were supported by grants from the Swedish Research Council (VR 2021-04938) and Kempestiftelserna (SMK21-0041). This work was also supported by Umeå Plant Science Center with grants from the Knut and Alice Wallenberg Foundation (KAW 2016.0352 and KAW 2020.0240), the Swedish Governmental Agency for Innovation Systems (VINNOVA 2016-00504), and Bio4Energy, a Strategic Research Environment supported through the Swedish Government's Strategic Research Area initiative.

Conflicts of Interest

The authors declare no conflicts of interest.

Data Availability Statement

All the raw data generated for this study, along with the processed data and quantification, have been deposited at Zenodo and are publicly available as of the date of publication (10.5281/zenodo.14971281).

The code for the Q-Warg workflow is publicly available on github (github.com/VergerLab/Q-Warg), and the specific version used for this study has been archived at Zenodo and is publicly available as of the date of publication at (10.5281/zenodo.14973382).

Requests for further information and resources should be directed to and will be fulfilled by the corresponding author, Stephane Verger: stephane.verger@umu.se.

References

Anderson, C. T., and J. J. Kieber. 2020. "Dynamic Construction, Perception, and Remodeling of Plant Cell Walls." *Annual Review of Plant Biology* 71 (Volume 71, 2020): 39–69. https://doi.org/10.1146/annurev-arplant-081519-035846.

Anderson, C. T., and J. Pelloux. 2025. "The Dynamics, Degradation, and Afterlives of Pectins: Influences on Cell Wall Assembly and Structure, Plant Development and Physiology, Agronomy, and Biotechnology." *Annual Review of Plant Biology* 76: 85–113. https://doi.org/10.1146/annurev-arplant-083023-034055.

Antoniadi, I., V. Skalický, G. Sun, et al. 2022. "Fluorescence Activated Cell Sorting – A Selective Tool for Plant Cell Isolation and Analysis." *Cytometry. Part A: Journal of the International Society for Analytical Cytology* 101, no. 9: 725–736. Available at:. https://doi.org/10.1002/cyto.a.24461.

Atakhani, A., L. Bogdziewiez, and S. Verger. 2022. "Characterising the Mechanics of Cell–Cell Adhesion in Plants." *Quantitative Plant Biology* 3: e2. https://doi.org/10.1017/qpb.2021.16.

Baas, S., and V. Saggiomo. 2021. "Ender3 3D Printer Kit Transformed Into Open, Programmable Syringe Pump Set." *HardwareX* 10: e00219. https://doi.org/10.1016/j.ohx.2021.e00219.

Barciszewski, J., F. Massino, and B. F. C. Clark. 2007. "Kinetin—A Multiactive Molecule." *International Journal of Biological Macromolecules* 40, no. 3: 182–192. https://doi.org/10.1016/j.ijbiomac.2006.06.024.

Besten, M., M. Hendriksz, L. Michels, et al. 2025. "CarboTag: A Modular Approach for Live and Functional Imaging of Plant Cell Walls." *Nature Methods* 22: 1081–1090. https://doi.org/10.1038/s41592-025-02677-4.

Bidhendi, A. J., and A. Geitmann. 2016. "Relating the Mechanics of the Primary Plant Cell Wall to Morphogenesis." *Journal of Experimental Botany* 67, no. 2: 449–461. https://doi.org/10.1093/jxb/erv535.

Cano, E. L., J. M. Moguerza, and A. Redchuk. 2012. "Design of Experiments With R." In *Six Sigma With R: Statistical Engineering for Process Improvement*, edited by E. L. Cano, J. M. Moguerza, and A. Redchuk, 197–215. New York, NY: Springer New York. https://doi.org/10.1007/978-1-4614-3652-2_11.

Chang, W. J. Cheng, J. J. Allaire, Y. Xie, and J. McPherson 2024 'Shiny: Web Application Framework for R'. https://cran.r-project.org/web/packages/shiny/ (Accessed: 19 February 2025).

Chupeau, M.-C., F. Granier, O. Pichon, J. P. Renou, V. Gaudin, and Y. Chupeau. 2013. "Characterization of the Early Events Leading to Totipotency in an Arabidopsis Protoplast Liquid Culture by Temporal Transcript Profiling." *Plant Cell* 25, no. 7: 2444–2463. https://doi.org/10.1105/tpc.113.109538.

Collins, J. T., J. Knapper, J. Stirling, et al. 2020. "Robotic Microscopy for Everyone: The OpenFlexure Microscope." *Biomedical Optics Express* 11, no. 5: 2447–2460. https://doi.org/10.1364/BOE.385729.

Cosgrove, D. J. 2024. "Structure and Growth of Plant Cell Walls." *Nature Reviews Molecular Cell Biology* 25, no. 5: 340–358. https://doi.org/10.1038/s41580-023-00691-y.

Create Interactive Web Graphics via 'plotly.js' [R package plotly version 4.10.4] 2024. Comprehensive R Archive Network (CRAN). https://CRAN.R-project.org/package=plotly (Accessed: 19 February 2025).

Damm, B., and L. Willmitzer. 1988. "Regeneration of Fertile Plants From Protoplasts of Different *Arabidopsis thaliana* Genotypes." *Molecular and General Genetics MGG* 213, no. 1: 15–20. https://doi.org/10.1007/BF00333392.

de Mendiburu, F. 2023. 'agricolae: Statistical Procedures for Agricultural Research'. Accessed: 19 February 2025 https://cran.r-project.org/web/packages/agricolae/index.html.

Eine Methode zur Isolierung lebender Protoplasten/von John Af Klercker 1892. *Accessed: 6 February 2025* http://sammlungen.ub.uni-frankfurt.de/botanik/4449859.

Fruleux, A., S. Verger, and A. Boudaoud. 2019. "Feeling Stressed or Strained? A Biophysical Model for Cell Wall Mechanosensing in Plants." *Frontiers in Plant Science* 10: 757. https://doi.org/10.3389/fpls.2019.00757.

Gilliard, G., E. Huby, S. Cordelier, M. Ongena, S. Dhondt-Cordelier, and M. Deleu. 2021. "Protoplast: A Valuable Toolbox to Investigate Plant Stress Perception and Response." *Frontiers in Plant Science* 12: 749581. https://doi.org/10.3389/fpls.2021.749581.

He, Q., Y. E, and R. Li. 2025 "Protoplast Cell-Wall Regeneration: Unlocking New Potential for Genetic Improvement and Tree Breeding." *Plant, Cell and Environment* 48, no. 8: 5786–5788. https://doi.org/10.1111/pce.15537.

Hoffmann, N., S. King, A. L. Samuels, and H. E. McFarlane. 2021. "Subcellular Coordination of Plant Cell Wall Synthesis." *Developmental Cell* 56, no. 7: 933–948. https://doi.org/10.1016/j.devcel.2021.03.004.

Huh, H., D. Jayachandran, J. Sun, et al. 2025. "Time-Resolved Tracking of Cellulose Biosynthesis and Assembly During Cell Wall Regeneration in Live *Arabidopsis* Protoplasts." *Science Advances* 11, no. 12: eads6312. https://doi.org/10.1126/sciadv.ads6312.

Jayachandran, D., P. Smith, M. Irfan, et al. 2023. "Engineering and Characterization of Carbohydrate-Binding Modules for Imaging Cellulose Fibrils Biosynthesis in Plant Protoplasts." *Biotechnology and Bioengineering* 120, no. 8: 2253–2268. https://doi.org/10.1002/bit.28484.

Jeong, Y. Y., H. Y. Lee, S. W. Kim, Y. S. Noh, and P. J. Seo. 2021. "Optimization of Protoplast Regeneration in the Model Plant *Arabidopsis thaliana*." *Plant Methods* 17, no. 1: 21. https://doi.org/10.1186/s13007-021-00720-x.

Jiang, F., J. Zhu, and H.-L. Liu. 2013. "Protoplasts: A Useful Research System for Plant Cell Biology, Especially Dedifferentiation." *Protoplasma* 250, no. 6: 1231–1238. https://doi.org/10.1007/s00709-013-0513-z.

24754455, 2025, 7, Downloaded from https://onlinelibrary.wiley.com/doi/10.1002/pld3.70090 by Umea University, Wiley Online Library on [21/07/2025]. See the Terms and Conditions (https://onlinelibrary.wiley.com/terms-and-conditions) on Wiley Online Library for rules of use; OA articles are governed by the applicable Creative Commons License

Krasteva, G., V. Georgiev, and A. Pavlov. 2021. "Recent Applications of Plant Cell Culture Technology in Cosmetics and Foods." *Engineering in Life Sciences* 21, no. 3–4: 68–76. https://doi.org/10.1002/elsc.202000078.

Kuki, H., T. Higaki, R. Yokoyama, et al. 2017. "Quantitative Confocal Imaging Method for Analyzing Cellulose Dynamics During Cell Wall Regeneration in *Arabidopsis* Mesophyll Protoplasts." *Plant Direct* 1, no. 6: e00021. https://doi.org/10.1002/pld3.21.

Kuki, H., R. Yokoyama, T. Kuroha, and K. Nishitani. 2020. "Xyloglucan Is Not Essential for the Formation and Integrity of the Cellulose Network in the Primary Cell Wall Regenerated From Arabidopsis Protoplasts." *Plants* 9, no. 5: 629. https://doi.org/10.3390/plants9050629.

Kumari, I. 2019. "A Simple Procedure for Isolation, Culture of Protoplast and Plant Regeneration." In *In Vitro Plant Breeding Towards Novel Agronomic Traits*, edited by M. Kumar et al., 263–273. Springer Singapore. https://doi.org/10.1007/978-981-32-9824-8_14.

Laforest, L. C., and S. S. Nadakuduti. 2022. "Advances in Delivery Mechanisms of CRISPR Gene-Editing Reagents in Plants." *Frontiers in Genome Editing* 4: 830178. https://doi.org/10.3389/fgeed.2022.830178.

Legland, D., I. Arganda-Carreras, and P. Andrey. 2016. "MorphoLibJ: Integrated Library and Plugins for Mathematical Morphology With ImageJ." *Bioinformatics* 32, no. 22: 3532–3534. https://doi.org/10.1093/bioinformatics/btw413.

Leszczuk, A., P. Kalaitzis, J. Kulik, and A. Zdunek. 2023. "Review: Structure and Modifications of Arabinogalactan Proteins (AGPs)." *BMC Plant Biology* 23, no. 1: 45. https://doi.org/10.1186/s12870-023-04066-5.

Masson, J., and J. Paszkowski. 1992. "The Culture Response of *Arabidopsis thaliana* Protoplasts Is Determined by the Growth Conditions of Donor Plants." *Plant Journal* 2, no. 5: 829–833. https://doi.org/10.1111/j.1365-313X.1992.tb00153.x.

Matsuo, S., A. Takenaga, T. Seyama, and T. Kondo. 2014. "Secretion of a Bundle of (1→3)-β-Glucan Hollow Fibrils From Protoplasts of Callus Suspension Under a Ca2+−Rich and Acidic Stressed Condition." *Holzforschung* 68, no. 1: 69–73. https://doi.org/10.1515/hf-2013-0010.

McKenna, J. F., A. F. Tolmie, and J. Runions. 2014. "Across the Great Divide: The Plant Cell Surface Continuum." *Current Opinion in Plant Biology* 22: 132–140. https://doi.org/10.1016/j.pbi.2014.11.004.

Ménard, D., H. Serk, R. Decou, and E. Pesquet. 2017. "Establishment and Utilization of Habituated Cell Suspension Cultures for Hormone-Inducible Xylogenesis." In *Xylem: Methods and Protocols*, edited by M. de Lucas and J. P. Etchhells, 37–57. Springer. https://doi.org/10.1007/978-1-4939-6722-3_4.

Ménard, D., H. Serk, R. Decou, and E. Pesquet. 2024. "Inducible Pluripotent Suspension Cell Cultures (iPSCs) to Study Plant Cell Differentiation." In *Xylem: Methods and Protocols*, edited by J. Agusti, 171–200. Springer US. https://doi.org/10.1007/978-1-0716-3477-6_13.

Menges, M., and J. A. H. Murray. 2002. "Synchronous Arabidopsis Suspension Cultures for Analysis of Cell-Cycle Gene Activity." *Plant Journal* 30, no. 2: 203–212. https://doi.org/10.1046/j.1365-313X.2002.01274.x.

Mukundan, N. S., K. Satyamoorthy, and V. S. Babu. 2025. "Advancing Plant Protoplasts: Innovative Techniques and Future Prospects." *Plant Biotechnology Reports* [Preprint]. https://doi.org/10.1007/s11816-025-00957-1.

Nagata, T., and I. Takebe. 1970. "Cell Wall Regeneration and Cell Division in Isolated Tobacco Mesophyll Protoplasts." *Planta* 92, no. 4: 301–308.

Nolan, R., L. Alvarez, S. Padilla-Parra, and G. Landini. 2023. 'autothresholdr: An R Port of the "ImageJ" Plugin "Auto Threshold"'. https://cran.r-project.org/web/packages/autothresholdr/index.html (Accessed: 19 February 2025).

Oda, Y., S. Asatsuma, H. Nakasone, and K. Matsuoka. 2020. "Sucrose Starvation Induces the Degradation of Proteins in Trans-Golgi Network and Secretory Vesicle Cluster in Tobacco BY-2 Cells." *Bioscience, Biotechnology, and Biochemistry* 84, no. 8: 1652–1666. https://doi.org/10.1080/09168451.2020.1756736.

Ooms, J. 2024. 'magick: Advanced Graphics and Image-Processing in R'. Accessed: 19 February 2025 https://cran.r-project.org/web/packages/magick/index.html.

Paredez, A. R., C. R. Somerville, and D. W. Ehrhardt. 2006. "Visualization of Cellulose Synthase Demonstrates Functional Association With Microtubules." *Science* 312, no. 5779: 1491–1495. https://doi.org/10.1126/science.1126551.

Park, Y. B., and D. J. Cosgrove. 2012. "A Revised Architecture of Primary Cell Walls Based on Biomechanical Changes Induced by Substrate-Specific Endoglucanases." *Plant Physiology* 158, no. 4: 1933–1943. https://doi.org/10.1104/pp.111.192880.

Pasternak, T., K. Lystvan, A. Betekhtin, and R. Hasterok. 2020. "From Single Cell to Plants: Mesophyll Protoplasts as a Versatile System for Investigating Plant Cell Reprogramming." *International Journal of Molecular Sciences* 21, no. 12: 4195. https://doi.org/10.3390/ijms21124195.

Pasternak, T., I. A. Paponov, and S. Kondratenko. 2021. "Optimizing Protocols for *Arabidopsis* Shoot and Root Protoplast Cultivation." *Plants* 10, no. 2: 375. https://doi.org/10.3390/plants10020375.

Peng, L., X. Gao, L. Wang, et al. 2022. "Design of Experiment Techniques for the Optimization of Chromatographic Analysis Conditions: A Review." *Electrophoresis* 43, no. 18–19: 1882–1898. https://doi.org/10.1002/elps.202200072.

Pesquet, E., A. V. Korolev, G. Calder, and C. W. Lloyd. 2010. "The Microtubule-Associated Protein AtMAP70-5 Regulates Secondary Wall Patterning in *Arabidopsis* Wood Cells." *Current Biology* 20, no. 8: 744–749. https://doi.org/10.1016/j.cub.2010.02.057.

Pesquet, E., A. Wagner, and J. H. Grabber. 2019. "Cell Culture Systems: Invaluable Tools to Investigate Lignin Formation and Cell Wall Properties." *Current Opinion in Biotechnology* 56: 215–222. https://doi.org/10.1016/j.copbio.2019.02.001.

Purushotham, P., R. Ho, and J. Zimmer. 2020. "Architecture of a Catalytically Active Homotrimeric Plant Cellulose Synthase Complex." *Science* 369, no. 6507: 1089–1094. https://doi.org/10.1126/science.abb2978.

Reed, K. M., and B. O. R. Bargmann. 2021. "Protoplast Regeneration and Its Use in New Plant Breeding Technologies." *Frontiers in Genome Editing* 3: 734951. https://doi.org/10.3389/fgeed.2021.734951.

Reyna-Llorens, I., M. Ferro-Costa, and S. J. Burgess. 2023. "Plant Protoplasts in the Age of Synthetic Biology." *Journal of Experimental Botany* 74, no. 13: 3821–3832. https://doi.org/10.1093/jxb/erad172.

Sakai, K., F. Charlot, T. le Saux, et al. 2019. "Design of a Comprehensive Microfluidic and Microscopic Toolbox for the Ultra-Wide Spatio-Temporal Study of Plant Protoplasts Development and Physiology." *Plant Methods* 15, no. 1: 79. https://doi.org/10.1186/s13007-019-0459-z.

Sakamoto, Y., A. Kawamura, T. Suzuki, et al. 2022. "Transcriptional Activation of Auxin Biosynthesis Drives Developmental Reprogramming of Differentiated Cells." *Plant Cell* 34, no. 11: 4348–4365. https://doi.org/10.1093/plcell/koac218.

Sapala, A., A. Runions, A. L. Routier-Kierzkowska, et al. 2018. "Why Plants Make Puzzle Cells, and How Their Shape Emerges." *eLife* 7: e32794. https://doi.org/10.7554/eLife.32794.

Sasamoto, H., S. Ogita, N. Hayashi, Y. Wakita, S. Yokota, and N. Yoshizawa. 2003. "Development of Novel Elongated Fiber-Structure in Protoplast Cultures of *Betula platyphylia* and *Larix leptolepis*." *In Vitro*

24754455, 2025, 7, Downloaded from https://onlinelibrary.wiley.com/doi/10.1002/pld3.70090 by Umea University, Wiley Online Library on [21/07/2025]. See the Terms and Conditions (https://onlinelibrary.wiley.com/terms-and-conditions) on Wiley Online Library for rules of use; OA articles are governed by the applicable Creative Commons License

Cellular and Developmental Biology - Plant 39, no. 2: 223–228. https://doi.org/10.1079/IVP2002388.

Schindelin, J., I. Arganda-Carreras, E. Frise, et al. 2012. "Fiji: An Open-Source Platform for Biological-Image Analysis." *Nature Methods* 9, no. 7: 676–682. https://doi.org/10.1038/nmeth.2019.

Schirawski, J., S. Planchais, and A.-L. Haenni. 2000. "An Improved Protocol for the Preparation of Protoplasts From an Established *Arabidopsis thaliana* Cell Suspension Culture and Infection With RNA of Turnip Yellow Mosaic Tymovirus: A Simple and Reliable Method." *Journal of Virological Methods* 86, no. 1: 85–94. https://doi.org/10.1016/S0166-0934(99)00173-1.

Seyama, T., and T. Kondo. 2012. "Morphological Responses of *Betula* Protoplasts in Fiber Spinning." *Holzforschung* 66, no. 3: 407–411. https://doi.org/10.1515/hf.2011.158.

Stringer, C., and M. Pachitariu. 2025. "Cellpose3: One-Click Image Restoration for Improved Cellular Segmentation." *Nature Methods* 22: 592–599. https://doi.org/10.1038/s41592-025-02595-5.

Suda, J., P. Kron, B. C. Husband, and P. Trávníček. 2007. "Flow Cytometry and Ploidy: Applications in Plant Systematics, Ecology and Evolutionary Biology." In *Flow Cytometry With Plant Cells*, 103–130. John Wiley & Sons, Ltd. https://doi.org/10.1002/9783527610921.ch5.

Tagawa, S., and T. Kondo. 2018. "Secretion of a Callose Hollow Fiber From Herbaceous Plant Protoplasts Induced by Inhibition of Cell Wall Formation." *Journal of Wood Science* 64, no. 5: 467–476. https://doi.org/10.1007/s10086-018-1726-8.

Tagawa, S., Y. Yamagishi, U. Watanabe, R. Funada, and T. Kondo. 2019. "Dynamics of Structural Polysaccharides Deposition on the Plasma-Membrane Surface of Plant Protoplasts During Cell Wall Regeneration." *Journal of Wood Science* 65, no. 1: 47. https://doi.org/10.1186/s10086-019-1826-0.

Tan, L., S. Eberhard, S. Pattathil, et al. 2013. "An Arabidopsis Cell Wall Proteoglycan Consists of Pectin and Arabinoxylan Covalently Linked to an Arabinogalactan Protein[W]." *Plant Cell* 25, no. 1: 270–287. https://doi.org/10.1105/tpc.112.107334.

Van Leene, J., D. Eeckhout, G. Persiau, et al. 2011. "Isolation of Transcription Factor Complexes From Arabidopsis Cell Suspension Cultures by Tandem Affinity Purification." In *Plant Transcription Factors: Methods and Protocols*, edited by L. Yuan and S. E. Perry, 195–218. Humana Press. https://doi.org/10.1007/978-1-61779-154-3_11.

Verma, A., M. Verma, and A. Singh. 2020. "Chapter 14 – Animal Tissue Culture Principles and Applications." In *Animal Biotechnology*, edited by A. S. Verma and A. Singh, Second ed., 269–293. Academic Press. https://doi.org/10.1016/B978-0-12-811710-1.00012-4.

Wickham, H., M. Averick, J. Bryan, et al. 2019. "Welcome to the Tidyverse." *Journal of Open Source Software* 4, no. 43: 1686. https://doi.org/10.21105/joss.01686.

Wu, F.-H., S. C. Shen, L. Y. Lee, S. H. Lee, M. T. Chan, and C. S. Lin. 2009. "Tape-Arabidopsis Sandwich - A Simpler Arabidopsis Protoplast Isolation Method." *Plant Methods* 5, no. 1: 16. https://doi.org/10.1186/1746-4811-5-16.

Xu, Y., R. Li, H. Luo, et al. 2022. "Protoplasts: Small Cells With Big Roles in Plant Biology." *Trends in Plant Science* 27, no. 8: 828–829. https://doi.org/10.1016/j.tplants.2022.03.010.

Yokoyama, R., H. Kuki, T. Kuroha, and K. Nishitani. 2016. "Arabidopsis Regenerating Protoplast: A Powerful Model System for Combining the Proteomics of Cell Wall Proteins and the Visualization of Cell Wall Dynamics." *Proteomes* 4, no. 4: 34. https://doi.org/10.3390/proteomes4040034.

Yokoyama, R., N. Shinohara, R. Asaoka, H. Narukawa, and K. Nishitani. 2014. "The Biosynthesis and Function of Polysaccharide Components of the Plant Cell Wall." In *Plant Cell Wall Patterning and Cell Shape*, 1–34. John Wiley & Sons, Ltd. https://doi.org/10.1002/9781118647363.ch1.

Yoo, S.-D., Y.-H. Cho, and J. Sheen. 2007. "Arabidopsis Mesophyll Protoplasts: A Versatile Cell System for Transient Gene Expression Analysis." *Nature Protocols* 2, no. 7: 1565–1572. https://doi.org/10.1038/nprot.2007.199.

Yue, J.-J., J. L. Yuan, F. H. Wu, et al. 2021. "Protoplasts: From Isolation to CRISPR/Cas Genome Editing Application." *Frontiers in Genome Editing* 3: 717017. https://doi.org/10.3389/fgeed.2021.717017.

Zhai, Z., H. Jung, and O. K. Vatamaniuk. 2009. "Isolation of Protoplasts From Tissues of 14-Day-Old Seedlings of *Arabidopsis thaliana*." *Journal of Visualized Experiments : JoVE* 30: 1149. https://doi.org/10.3791/1149.

Zhang, S., T. Zhang, S. Wang, Z. Han, X. Duan, and J. Wang. 2024. "Phenotyping of Single Plant Cells on a Microfluidic Cytometry Platform With Fluorescent, Mechanical, and Electrical Modules." *Analyst* 149, no. 17: 4436–4442. https://doi.org/10.1039/d4an00682h.

Supporting Information

Additional supporting information can be found online in the Supporting Information section.

24754455, 2025, 7, Downloaded from https://onlinelibrary.wiley.com/doi/10.1002/pld3.70090 by Umea University, Wiley Online Library on [21/07/2025]. See the Terms and Conditions (https://onlinelibrary.wiley.com/terms-and-conditions) on Wiley Online Library for rules of use; OA articles are governed by the applicable Creative Commons License